Mon. Not. R. Astron. Soc. **000**, 1–23 (2007) Printed 1 February 2008 (MN LaTeX style file v2.2)

Astrophysical Configurations with Background Cosmology: Probing Dark Energy at Astrophysical Scales

A. Balaguera-Antolínez[1⋆], D. F. Mota[2]† and M. Nowakowski[3]‡
[1] *Max Planck Institute für Extraterrestrische Physik, D-85748, Garching, Germany*
[2] *Institute for Theoretical Physics, University of Heidelberg, 69120 Heidelberg, Germany*
[3] *Departamento de Física, Universidad de los Andes, A.A. 4976, Bogotá, D.C., Colombia*

1 February 2008

ABSTRACT
We explore the effects of a positive cosmological constant on astrophysical and cosmological configurations described by a polytropic equation of state. We derive the conditions for equilibrium and stability of such configurations and consider some astrophysical examples where our analysis may be relevant. We show that in the presence of the cosmological constant the isothermal sphere is not a viable astrophysical model since the density in this model does not go asymptotically to zero. The cosmological constant implies that, for polytropic index smaller than five, the central density has to exceed a certain minimal value in terms of the vacuum density in order to guarantee the existence of a finite size object. We examine such configurations together with effects of Λ in other exotic possibilities, such as neutrino and boson stars, and we compare our results to N-body simulations. The astrophysical properties and configurations found in this article are specific features resulting from the existence of a dark energy component. Hence, if found in nature would be an independent probe of a cosmological constant, complementary to other observations.

Key words: Cosmology – Theory – Dark Energy – Structure Formation

1 INTRODUCTION

Some of the most relevant properties of the universe have been established through astronomical data associated to light curves of distant Supernova Ia (Riess et al. 2004), the temperature anisotropies in the cosmic microwave background radiation (Spergel et al. 2006) and the matter power spectrum of large scale structures (Tegmark et al. 2004). Such observations give a strong evidence that the geometry of the universe is flat and that our Universe is undertaking an accelerated expansion at the present epoch. This acceleration is attributed to a dominant dark energy component, whose most popular candidate is the cosmological constant, Λ.

The present days dominance of dark energy make us wonder if this component may affect the formation and stability of large astrophysical structures, whose physics is basically Newtonian. This is in fact an old question put forward already by Einstein (Einstein & Straus 1945) and pursued by many other authors (Noerdlinger & Petrosian 1971; Chernin Nagirner & Starikova 2003; Manera & Mota 2005; Nunes & Mota 2006; Baryshev,Chernin & Teerikorpi 2001) and (Kagramanova,Kunz & Laemmerzahl 2006; Jetzer & Serena 2006). In general, the problem is rooted in the question whether the expansion of the universe, which in the Newtonian sense could be understood as a repulsive force, affects local astrophysical properties of large objects. The answer is certainly affirmative if part of the terms responsible for the Universe expansion survives the Newtonian limit of the Einstein equations. This is indeed the case of Λ which is part of the Einstein tensor. In fact, as explained in the main text below, all the effects of the universe expansion can be taken into account, regardless of the model, by generalizing the Newtonian limit. This approach allow us to calculate the impact of a given cosmological model on astrophysical structures.

⋆ E-mail: abalan@mpe.mpg.de
† E-mail: d.mota@thphys.uni-heidelberg.de
‡ E-mail: mnowakos@uniandes.edu.co

Although, there are several candidates to dark energy which have their own cosmological signature, e.g. (Koivisto & Mota 2007; Daly & Djorgovski 2004; Wang & Mukherjee 2004; Koivisto & Mota 2006; Koivisto & Mota 2007a; Mota & Shaw 2007) and (Seo & Eisenstein 2003; Brookfield et al. 2006; Daly & Djorgovski 2003; Koivisto & Mota 2007b; Mota & Shaw 2006), in this paper we will investigate the ΛCDM model only. Such consideration is in fact not restrictive and our results will be common to most dark energy models. At astrophysical scales and within the Newtonian limit one does not expect to find important differences among the different dark energy models. This, however should not be interpreted as if Λ has no effect at smaller astrophysical scales. In fact, the effects of a cosmological constant on the equilibrium and stability of astrophysical structures is not negligible, and can be of relevance to describe features of astrophysical systems such as globular clusters, galaxy clusters or even galaxies (Chernin et al. 2007; Iorio 2005; Balaguera-Antolínez,Böhmer & Nowakowski 2006b; Nowakowski & Sanabria & Garcia 2002; Cardoso & Gualtieri 2006). Motivated by this, we investigate the effects of a dark energy component on the Newtonian limit of Einstein gravity and its consequences at astrophysical scales.

In this article we investigate how the cosmological constant changes certain aspects of astrophysical hydrostatic equilibrium. In particular we search for specific imprints which are unique to the existence of a dark energy fluid. For instance, the instability of previously viable astrophysical models when Λ is included. We explore such possibility using spherical configurations described by a polytropic equation of state (e.o.s) $p \sim \rho^{\gamma}$. The polytropic equation of state derives its importance from its success and consistency, and it is widely used in determining the properties of gravitational structures ranging from stars (Chandrasekhar 1967) to galaxies (Binney & Tremaine 1987). It leads to an acceptable description of the behavior of astrophysical objects in accordance with observations and numerical simulations (Kennedy & Bludman 1999; Gruzinov 2000; Kaniadakis,Lavagno & Quarati 1996; Sadeth & Rephaeli 2004; Pinzon & Calvo-Mozo 2001; Ruffet et al. 1996). The description of such configurations can be verified in the general relativistic framework (Herrera & Barreto 2003) and applications of these models to the dark energy problem have in fact been explored (Mukhopadhyay & Ray 2005).

The effect of a positive cosmological constant can be best visualized as a repulsive non local force acting on the matter distribution. It is clear that this extra force will result into a minimum density (either central or average) which is possible for the distribution to be in equilibrium. This minimum density is a crucial crossing point: below this value no matter can be in equilibrium, above this value low density objects exist (Lahav et al. 1991). Both effects are novel features due to Λ. We will demonstrate such inequalities, which are generalizations of corresponding inequalities found in (Nowakowski & Sanabria & Garcia 2002) and (Balaguera-Antolínez,Böhmer & Nowakowski 2005a), for every polytropic index n. However, the most drastic effect can be found in the limiting case of the polytropic equation of state, i.e, the isothermal sphere where the polytropic index n goes to infinity. This case captures, as far as the effects of Λ are concerned, many features also for higher, but finite n. The model of the isothermal sphere is often used to model galaxies and galactic clusters (Natarajan & Lynden-Bell 1997) and used in describing effects of gravitational lensing (Kawano et al. 2004; Sereno 2005; Maccio 2004). Herein lies the importance of the model. Regarding the isothermal sphere we will show that Λ renders the model unacceptable on general grounds. This essentially means that the model does not even have an appealing asymptotic behavior for large radii and any attempt to definite a physically acceptable radius has its severe drawbacks.

The positive cosmological constant offers, however, yet another unique opportunity, namely the possible existence of young low density virialized objects, understood as configurations that have reached virial equilibrium just at the vacuum dominated epoch (in contrast to the structures forming during the matter dominated era, where the criteria for virialization is roughly $\bar{\rho} \approx 200\rho_{\rm crit}$). This low density hydrostatic/virialized objects can be explained again due to Λ which now partly plays the role of the outward pressure.

The applicability of fluid models, virial theorem and hydrostatic equilibrium to large astrophysical bodies has been discussed many times in the literature. For a small survey on this topic we refer the reader to (Jackson 1970; Balaguera-Antolínez,Mota & Nowako
where one can also find the relevant references.

It is interesting to notice that dark matter halos represent a constant density background which, in the Newtonian limit, objects embedded in them feel the analog to a negative cosmological constant. The equilibrium analysis for such configurations has been performed in (Umemura & Ikeuchi 1986; Horedt 2000). A negative Λ will just enhance the attractive gravity effect, whereas a positive one opposes this attraction. As a result the case $\Lambda > 0$ reveals different physical concepts as discussed in this paper.

The article is organized as follows. In the next section we introduce the equations relevant for astrophysical systems as a result of the weak field limit and the non-relativistic limit of Einstein field equations taking into account a cosmological constant. There we derive such limit taking into account the background expansion independently of the dark energy model. In section 3 we derive the equations governing polytropic configurations, the equilibrium conditions and stability criteria. In section 4 we describe the isothermal sphere and investigate its applicability in the presence of Λ. In section 5 we explore some examples of astrophysical configurations where the cosmological constant may play a relevant role. In particular, we probe into low density objects, fermion (neutrino) stars and boson stars. Finally we perform an important comparison between polytropic configurations with Λ and parameterized density of Dark Matter Halos. We end with conclusions. We use units $G_N = c = 1$ except in section 5.4 where we restore G_N and use natural units $\hbar = c = 1$.

2 LOCAL DYNAMICS IN THE COSMOLOGY BACKGROUND

The dynamics of the isotropic and homogeneous cosmological background is determined by the evolution of the (dimensionless) scale factor given through the Friedman-Robertson-Walker line element as solution of Einstein field equations,

$$\frac{\ddot{a}(t)}{a(t)} = -\frac{4}{3}\pi\left[\rho(t) + 3p(t)\right], \qquad \left[\frac{\dot{a}(t)}{a(t)}\right]^2 = H(t)^2 = \frac{8}{3}\pi\rho(t) - \frac{k}{a^2(t)}, \tag{1}$$

corresponding to the Raychaudhury equation and Friedman equation, respectively. The total energy density ρ is a contribution from a matter component - baryonic plus dark matter - ($\rho_{\rm mat} \sim a^{-3}$), radiation ($\rho_{\rm rad} \sim a^{-4}$) and a dark energy component ($\rho_{\rm x} \sim a^{-f(a)}$ with $p = \omega_{\rm x}\rho$). The function $f(a)$ is given as

$$f(a) \equiv \frac{3}{\ln a}\int_1^a \frac{\omega_{\rm x}(a') + 1}{a'}{\rm d}a', \tag{2}$$

where the term $\omega_{\rm x}(a)$ represents the equation of state for the dark energy component. The case $\omega_{\rm x} = -1$ corresponds to the cosmological constant $\rho_{\rm x} = \rho_{\rm vac} = \Lambda/8\pi$. The effects of the background on virialized structures can be explored through the Newtonian limit of field equations from which one can derive a modified Poisson's equation (see e.g. (Noerdlinger & Petrosian 1971; Nowakowski 2001)). Recalling that pressure is also a source for gravity, the gravitational potential produced by an overdensity is given by

$$\nabla^2\Phi = 4\pi(\rho_t + 3P_t), \tag{3}$$

where $\rho_t = \delta\rho + \rho$ and $P_t = \delta P + P$. Where $\delta\rho$ is the local overdensity with respect to the background density ρ. Notice that equation (3) reduces to the usual Poisson equation, $\nabla^2\Phi = 4\pi\delta\rho$, when non relativistic matter dominates the Universe, and $\delta\rho \gg \rho$. However, at present times, when dark energy dominates, the pressure is non-negligible and δP might even be non zero, such as in the case of quintessence models (Maor & Lahav 2005; Wang & Steinhardt 1998; Mota & van de Bruck 2004). In this work, however, we will focus in the case of an homogeneous dark energy component where $\delta\rho = \delta P = 0$. With this in mind, one can then write the modified Poisson equation as

$$\nabla^2\Phi = 4\pi\delta\rho - 3\frac{\ddot{a}(t)}{a(t)}, \tag{4}$$

Note that this equation allows one to probe local effects of different Dark Energy models through the term $\ddot{a}/a$ given in Eq.(1).

Since we will be investigating the configuration and stability of astrophysical objects nowadays, when dark energy dominates, it is more instructive to write the above equations in terms of an effective vacuum density i.e.

$$\nabla^2\Phi = 4\pi\delta\rho - 8\pi\rho_{\rm vac}^{\rm eff}(a), \tag{5}$$

where by using (1) $\rho_{\rm vac}^{\rm eff}(a)$ has been defined as

$$\rho_{\rm vac}^{\rm eff}(a) \equiv -\frac{1}{2}\left[\left(\frac{\Omega_{\rm cdm}}{\Omega_{\rm vac}}\right)a^{-3} + (1+3\omega_{\rm x})a^{-f(a)}\right]\rho_{\rm vac}, \tag{6}$$

which reduces to $\rho_{\rm vac}$ for $\omega_{\rm x} = -1$ and negligible contribution from the cold dark matter component with respect to the overdensity $\delta\rho$. With $\Phi_{\rm grav}$ being the solution associated to the pure gravitational interaction, the full solution for the potential can be simply written as

$$\Phi(r,a) = \Phi_{\rm grav}(r) - \frac{4}{3}\pi\rho_{\rm vac}^{\rm eff}(a)r^2, \qquad \Phi_{\rm grav}(r) = -\int_{V'}\frac{\delta\rho(\mathbf{r}')}{|\mathbf{r}-\mathbf{r}'|}\,{\rm d}^3{\rm r}', \tag{7}$$

which defines the Newton-Hooke space-time for a scale factor close to the present time (vacuum dominated epoch), $\omega_{\rm x} = -1$ and $\Omega_{\rm cdm} \ll \Omega_{\rm vac}$ (Gibbons & Patricot 2003; Aldrovandi et al.1998). For a ΛCDM universe with $\Omega_{\rm cdm} = 0.27$ and $\Omega_{\rm vac} = 0.73$ we get $\rho_{\rm vac}^{\rm eff}(\text{today}) = 0.81\rho_{\rm vac}$: that is, the positive density of matter which has an attractive effect opposing the repulsive one of Λ reduces effectively the strength of the 'external force' in (5). Note that, although in the text we will use the notation $\rho_{\rm vac}$ which would be vaild in the case of a Newton-Hook space time, it must be understood that we can replace $\rho_{\rm vac}$ by $\rho_{\rm vac}^{\rm eff}(\text{today}) = 0.81\rho_{\rm vac}$ for a ΛCDM background.

Given the potential $\Phi(r,a)$, we can write the Euler's equation for a self-gravitating configuration as

$$\rho\frac{d\langle v_i\rangle}{dt} + \partial_i p + \rho\partial_i\Phi = 0$$

, where $\langle v_i\rangle$ is the (statistical) mean velocity and ρ is the total energy density in the system. We can go beyond Euler's equation and write down the tensor virial equation which reduces to its scalar version for spherical configurations. The (scalar) virial equation with the background contribution reads as (Balaguera-Antolínez & Nowakowski 2005; Caimmi 2007)

$$\frac{{\rm d}^2\mathcal{I}}{{\rm d}t^2} = 2T + \mathcal{W}^{\rm grav} + 3\Pi + \frac{8}{3}\pi\rho_{\rm vac}^{\rm eff}(a)\mathcal{I} - \int_{\partial V} p\,(\vec{r}\cdot\hat{n})\,{\rm d}A, \tag{8}$$

where $\mathcal{W}^{\rm grav}$ is the gravitational potential energy defined by

$$\mathcal{W}^{\rm grav} = \frac{1}{2}\int_V \rho(\mathbf{r})\Phi_{\rm grav}(\mathbf{r}){\rm d}^3{\rm r}, \tag{9}$$

and $T = \frac{1}{2}\int_V \rho\langle v^2\rangle {\rm d}^3{\rm r}$ is the contribution of ordered motions to the kinetic energy. Also, $\mathcal{I} \equiv \int_V \rho r^2 {\rm d}^3{\rm r}$ is the moment of inertia about the center of the configuration and $\Pi \equiv \int_V p{\rm d}^3{\rm r}$ is the trace of the dispersion tensor. The full description of a self gravitating configuration is completed with an equation for mass conservation, energy conservation and an equation of state $p = p(\delta\rho, s)$. If we assume equilibrium via $\ddot{\mathcal{I}} \approx 0$, we obtain the known virial theorem (Jackson 1970; Balaguera-Antolínez & Nowakowski 2005)

$$|\mathcal{W}^{\rm grav}| = 2T + 3\Pi + \frac{8}{3}\pi\rho_{\rm vac}^{\rm eff}(a)\mathcal{I}, \tag{10}$$

where we have neglected the surface term in (8), which is valid in the case when we define the boundary of the configuration where $p = 0$.

With $\rho_{\rm vac}^{\rm eff}$ given in (6), one must be aware that an equilibrium configuration is at the most a dynamical one. This is to say that the 'external repulsive force' in (6) is time dependent through the inclusion of the background expansion and so are the terms in (8). This leads to a violation of energy conservation, which also occurs in the virialization process (Wang 2006; Maor & Lahav 2005; Caimmi 2007; Mota & van de Bruck 2004; Shaw & Mota 2007)). Traced over cosmological times, this implies that if we insist on the second derivative of the inertial tensor to be zero, then the internal properties of the object like angular velocity or the internal mean velocity of the components will change with time. Even if in the simplest case, one can assume that the objects shape and its density remain constant. Hence, equilibrium here can be thought of as represented by long time averages in which case the second derivative also vanishes, not because of constant volume and density, but because of stability (Balaguera-Antolínez & Nowakowski 2006; Balaguera-Antolínez,Mota & Nowakowski 2006).

The expressions derived in the last section, especially (5) and (10) can be used for testing dark energy models on configurations in a dynamical state of equilibrium. However, in these cases, one should point out that, in this approach there is no energy conservation within the overdensity: dark energy flows in and out of the overdensity. Such feature is a consequence of the assumption that dark energy does not cluster at small scales (homogeneity of dark energy). This is in fact the most common assumption in the literature(Wang & Steinhardt 1998; Chen & Ratra 2004; Horellou & Berge 2005), with a few exceptions investigated in (Wang 2006; Maor & Lahav 2005; Caimmi 2007; Mota & van de Bruck 2004).

In this paper, we will concentrate on the possible effects of a background dominated by a dark energy component represented by the cosmological constant at late times ($z \leqslant 1$). It implies that the total density involved in the definitions of the integral quantities appearing in the virial equation can be approximated to $\rho \sim \delta\rho$. In that case the Poisson equation reduces to the form $\nabla^2\Phi = 4\pi\delta\rho - 8\pi\rho_{\rm vac}$. As mentioned before, the symbol $\rho_{\rm vac}$ has no multiplicative factors in the case of a Newton-Hooke space time, while for a ΛCDM model it must be understood as $\rho_{\rm vac} \to 0.8\rho_{\rm vac}$. As the reader will see, the most relevant quantities derived here come in forms of ratio of a characterizing density and $\rho_{\rm vac}$, and hence the extra factor appearing in the ΛCDM can be re-introduced in the characterizing density. For general consideration of equilibrium in the spherical case see (Böhmer 2004) and (Böhmer & Harko 2005), while the quasi spherical collapse with cosmological constant has been discussed in (Debnath et al 2006).

3 POLYTROPIC CONFIGURATIONS AND THE Λ-LANE-EMDEN EQUATION

We can determine the relevant features of astrophysical systems by solving the dynamical equations describing a self gravitating configuration (Euler's equation, Poisson's equation, continuity equations). In order to achieve this goal we must first know the potential Φ to be able to calculate the gravitational potential energy. To obtain Φ, one must supply the density profile and solve Poisson's equation. In certain cases, the potential is given and we therefore can solve for the density profile in a simple way. Here we face the situation where no information on the potential (aside from its boundary conditions) is available and we also do not have an apriori information about the density profile (see for instance (Binney & Tremaine 1987) for related examples). In order to determine both, the potential and the density profile, a complete description of astrophysical systems required. This means we need to know an equation of state $p = p(\rho)$ (here we change notation and we call ρ the proper density of the system). The equation of state can take several forms and the most widely used one is the so-called *polytropic equation of state*, expressed as

$$p = \kappa\rho^{\gamma}, \qquad \gamma \equiv 1 + \frac{1}{n}, \tag{11}$$

where γ is the polytropic index and κ is a parameter that depends on the polytropic index, central density, the mass and the radius of the system. The exponent γ is defined as $\gamma = (c_{\rm p} - c)/(c_{\rm v} - c)$ and is associated with processes with constant (non-zero) specific heat c. It reduces to the adiabatic exponent if $c = 0$. The polytropic equation of state was introduced to model fully convective configurations. From a statistical point of view, Eq. (11) represents a collisionless system whose distribution function

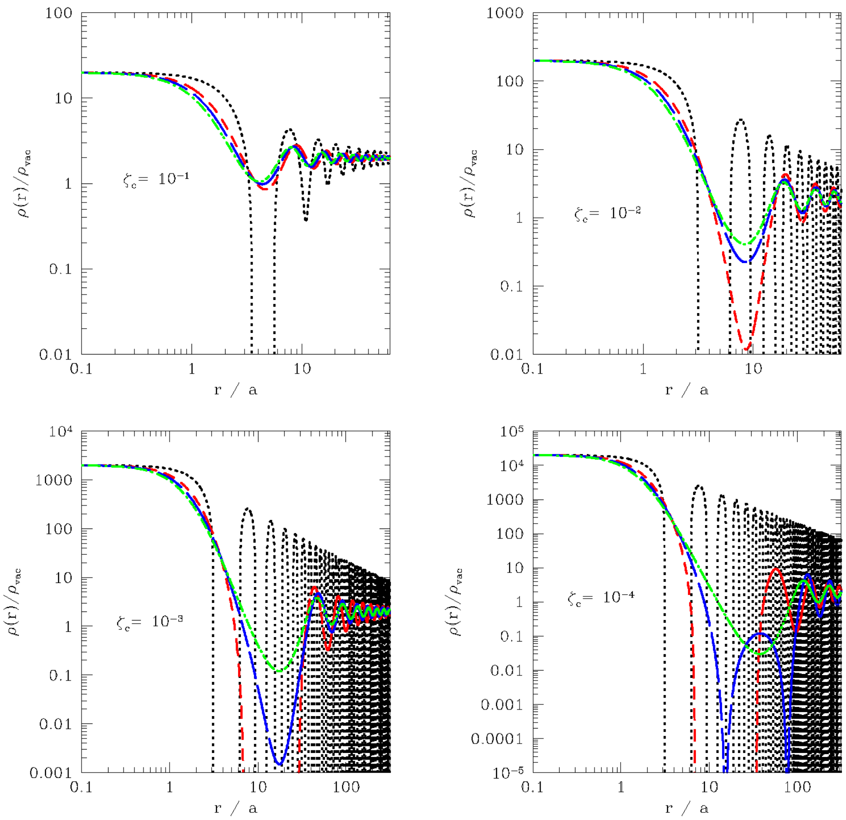

Figure 1. Solutions of ΛLE equation for different ζ_c and different index n ranging from $n = 3$ (red, short-dashed line), $n = 4$ (blue,long-dashed line) and $n = 5$ (green,dot short-dashed line).

can be written in the form $f = f(\tilde{E}) \sim \tilde{E}^{n-3/2}$, with $\tilde{E} \equiv \phi - (1/2)mv^2$ being the relative energy and $\phi(r) \equiv \Phi_0 - \Phi(r)$ being the relative potential (where Φ_0 is a constant chosen such that $\phi(r = R) = 0$)(Binney & Tremaine 1987). In astrophysical contexts, the polytropic equation of state is widely used to describe astrophysical systems such as the sun, compact objects, galaxies and galaxy clusters (Chandrasekhar 1967; Binney & Tremaine 1987; Kennedy & Bludman 1999). We now derive the well known Lane-Emden equation. We start from Poisson equation and Euler equation for spherically symmetric configurations, written as

$$\frac{\mathrm{d}^2\Phi}{\mathrm{d}r^2} + \frac{2}{r}\frac{\mathrm{d}\Phi}{\mathrm{d}r} = 4\pi\rho - 8\pi\rho_{\mathrm{vac}}, \qquad \frac{\mathrm{d}p}{\mathrm{d}r} = -\rho\frac{\mathrm{d}\Phi}{\mathrm{d}r}. \tag{12}$$

This set of equations together with Eq. (11) can be integrated in order to solve for the density in terms of the potential as

$$\rho(r) = \rho_{\mathrm{c}}\left[1 - \left(\frac{\gamma-1}{\kappa\gamma}\right)\rho_{\mathrm{c}}^{1-\gamma}(\Phi(r) - \Phi(0))\right]^{\frac{1}{\gamma-1}}, \tag{13}$$

where ρ_c is the central density. In view of eq. (13) in conjunction with eq. (7) it is clear that ρ_{vac} will have the effect to increase the value of $\rho(r)$. Therefore the boundary of the configuration will be located in a greater R as compared to the case $\rho_{\mathrm{vac}} = 0$. In order to determine the behavior of the density profile, we again combine Eq(12) and Eq.(11) in order to eliminate the potential $\Phi(r)$. We obtain

$$\frac{1}{n}\left(\frac{\nabla\rho}{\rho}\right)^2 + \nabla^2\ln\rho = -\frac{4\pi n\rho^{1-\frac{1}{n}}}{\kappa(n+1)}\left(1-\zeta\right), \tag{14}$$

where we defined the function

$$\zeta = \zeta(r) \equiv 2\left(\frac{\rho_{\mathrm{vac}}}{\rho(r)}\right). \tag{15}$$

We can rewrite Eq (14) by introducing the variable ψ defined by $\rho = \rho_{\rm c}\psi^{n}$, where $\rho_{\rm c}$ is the central density. We also introduce the variable $\xi = r/a$ where

$$a \equiv \sqrt{\frac{\kappa(n+1)}{4\pi\rho_{\rm c}^{1-\frac{1}{n}}}} \tag{16}$$

is a length scale. Eq.(14) is finally written as (Balaguera-Antolínez,Böhmer & Nowakowski 2005a; Chandrasekhar 1967)

$$\frac{1}{\xi^2}\frac{\mathrm{d}}{\mathrm{d}\xi}\left(\xi^2\frac{\mathrm{d}\psi}{\mathrm{d}\xi}\right) = \zeta_{\rm c} - \psi^{n}, \qquad \zeta_{\rm c} \equiv 2\left(\frac{\rho_{\rm vac}}{\rho_{\rm c}}\right). \tag{17}$$

This is the Λ-Lane-Emden equation (ΛLE). Note that for constant density, we recover $\rho = 2\rho_{\rm vac}$ as the first non trivial solution of ΛLE equation. This is consistent with the results from virial theorem for constant density spherical objects which tell us that $\rho \geqslant 2\rho_{\rm vac}$ (Nowakowski & Sanabria & Garcia 2002). Note that using Eq. (13) we can write the solution $\psi(\xi)$ with the explicit contribution of $\rho_{\rm vac}$ as

$$\psi\left(\xi = r/a\right) = 1 - \left(4\pi a^2\rho_{\rm c}\right)^{-1}\left(\Phi_{\rm grav}(r) - \Phi_{\rm grav}(0)\right) + 6\zeta_{\rm c}\xi^2, \tag{18}$$

so that for a given r smaller than the radius we will obtain

$$\psi\left(r/a\right) > \psi\left(r/a\right)_{\Lambda=0}, \tag{19}$$

as already pointed out before. Then the differential equation (17) must be solved with the initial conditions $\psi(0) = 1$, $\psi'(0) = 0$, satisfied by (18). Numerical solutions were obtained for the first time in (Balaguera-Antolínez & Nowakowski 2005). The solutions presented in Fig. 1 are given in terms of the ratio $\rho/\rho_{\rm vac}$ for $n = 3, 4$ and $n = 5$. This choice of variables are useful also since $\rho_{\rm vac}$ sets a fundamental scale of density (the choice $\rho_0 = \rho_{\rm vac}$ will be explored for the isothermal sphere, where figure 1 will be helpful for discussions). The radius of a polytropic configuration is determined as the value of r when the density of matter with the e.o.s (11) vanishes. This happens at a radius located at

$$R = a\xi_1 \;\text{ such that }\; \psi(\xi_1) = 0. \tag{20}$$

Note that equation (17) yields a transcendental equation to determine ξ_1. Also one notes from Fig. 1 that not all values of $\zeta_{\rm c}$ yield allowed configurations in the sense that we cannot find a value of ξ_1 such that $\psi(\xi_1) = 0$. This might not be surprising since for $n = 5$ and $\Lambda = 0$ we find the situation where the asymptotic behavior is $\rho \to 0$ as $\xi \to \infty$ (we consider this still as an acceptable behavior). There is, however, one crucial difference when we switch on a non-zero Λ. For $\Lambda \neq 0$ not only we cannot reach a definite radius but the derivative of the density changes sign and hence becomes non-physical. The situation for the cases $n \geqslant 5$ is somewhat similar to the extreme case of $n \to \infty$ (isothermal sphere). Clearly, these features are responsible of the last term in Eq.(18), which for high values of ζ may become dominant over the remaining (gravitational) terms. We will discuss this case in section four where we will attempt another definition of a finite radius with the constraint $\psi(\xi)' < 0$. For now it is sufficient to mention that, as expected, the radius of the allowed configurations are larger than the corresponding radius when $\Lambda = 0$.

3.1 Equilibrium and stability for polytropes

In this section we will derive the equilibrium conditions for polytropic configurations in the presence of a positive cosmological constant. We will use the results of last section in order to write down the virial theorem. The total mass of the configuration can be determined as usual with $M = \int \rho\,\mathrm{d}^3\mathrm{r}$ together with Eq.(17). One then has a relation between the mass, the radius and the central density:

$$R = M^{1/3}\rho_{\rm c}^{-1/3}f_0(\zeta_{\rm c};n) = (Mr_{\Lambda}^2)^{1/3}(4\pi)^{1/3}\zeta_{\rm c}^{1/3}f_0(\zeta_{\rm c};n) \tag{21}$$

where

$$f_0(\zeta_{\rm c};n) \equiv \left(\frac{\xi_1^3}{4\pi}\right)^{\frac{1}{3}}\left(\int_0^{\xi_1}\xi^2\psi^n(\xi)\mathrm{d}\xi\right)^{-\frac{1}{3}}, \tag{22}$$

Note that we have introduced the cosmological constant in the equation for the radius, leading to the appearance of the astrophysical length scale $\left(Mr_{\Lambda}^2\right)^{1/3}$ (with $r_{\Lambda} = \Lambda^{-1/2} = (8\pi\rho_{\rm vac})^{-1/2} = 2.4\times 10^3(\Omega_{\rm vac}h^2)^{-1/2}$Mpc $\approx 4.14\times 10^3$ Mpc for the concordance values $\Omega_{\rm vac} = 0.7$ and $h = 0.7$). This scale has been already found in the context of Schwarzschild - de Sitter metric where it is the maximum allowed radius for bound orbits. At the same time it is the scale of the maximum radius for a self gravitating spherical and homogeneous configuration in the presence of a positive Λ (Balaguera-Antolínez & Nowakowski 2005). This also let us relate the mean density of the configuration with its central density and/or cosmological parameters as $\bar{\rho} = (3/4\pi f_0^3)\rho_{\rm c} = (3/2\pi\zeta_{\rm c}f_0^3)\rho_{\rm vac} = (3\Omega_{\rm vac}/2\pi\zeta_{\rm c}f_0^3)\rho_{\rm crit}$.

Similarly we can determine the other relevant quantities appearing in the equations for the energy and the scalar virial theorem (10). For the traces of the moment of inertia tensor and the dispersion tensor Π we can write

$$\mathcal{I} = MR^2 f_1, \qquad \Pi = \kappa \rho_c^{\frac{1}{n}} M f_2, \tag{23}$$

where the functions $f_{1,2}$ have been defined as

$$f_1(\zeta_c; n) \equiv \frac{\int_0^{\xi_1} \xi^4 \psi^n \mathrm{d}\xi}{\xi_1^2 \int_0^{\xi_1} \xi^2 \psi^n \mathrm{d}\xi}, \qquad f_2(\zeta_c; n) \equiv \frac{\int_0^{\xi_1} \xi^2 \psi^{n+1} \mathrm{d}\xi}{\int_0^{\xi_1} \xi^2 \psi^n \mathrm{d}\xi}, \tag{24}$$

using (21). These functions are numerically determined in the sequence $\psi(\xi;\zeta_c) \to \xi_1(\zeta_c) \to f_i(\zeta_c)$, such that for a given mass we obtain the radius as $R = a(M;\xi_1)\xi_1$.

Let us consider the virial theorem (10) for a polytropic configuration. The gravitational potential energy $\mathcal{W}^{\mathrm{grav}}$ can be obtained following the same arguments shown in (Chandrasekhar 1967). The method consist in integrating Euler's equation and solve for Φ_{grav}, then using Eq.(9) one obtains $\mathcal{W}^{\mathrm{grav}}$. The final result is written as

$$\mathcal{W}^{\mathrm{grav}} = -\frac{M^2}{2R} - \frac{1}{2}(n+1)\Pi + \frac{2}{3}\pi\rho_{\mathrm{vac}}\left(\mathcal{I} - MR^2\right), \tag{25}$$

To show the behavior of $\mathcal{W}^{\mathrm{grav}}$ with respect to the index n, we can solve the the virial theorem (10) for Π and replace it in Eq.(25). We obtain

$$\mathcal{W}^{\mathrm{grav}} = -\frac{3}{5-n}\left[1 - \frac{\rho_{\mathrm{vac}}}{\bar{\rho}}\left(\frac{1}{3}(5+2n)f_1 - 1\right)\right]\frac{M^2}{R}. \tag{26}$$

This expression shows the typical behavior of a $n = 5$ polytrope (even if $\rho_{\mathrm{vac}} \neq 0$): the configuration has an infinite potential energy, due to the fact that the matter is distributed in a infinite volume. The energy of the configuration in terms of the polytropic index can be easily obtained by using (10), (25) and (26)

$$E = \mathcal{W}^{\mathrm{grav}} + \frac{8}{3}\pi\rho_{\mathrm{vac}}\mathcal{I} + n\Pi = -\left(\frac{3-n}{5-n}\right)\frac{M^2}{R}\left[1 - \frac{\rho_{\mathrm{vac}}}{\bar{\rho}}\left(5f_1^{(n)} - 1\right)\right]. \tag{27}$$

One is tempted to use $E < 0$ as the condition to be fulfilled for a gravitationally bounded system. For $\rho_{\mathrm{vac}} = 0$ we recover the condition $\gamma > 4/3$ ($n < 3$) for gravitationally bounded configurations in equilibrium. On the other hand, for $\rho_{\mathrm{vac}} \neq 0$ this condition might not be completely true due to the following reasoning: The two-body effective potential in the presence of a positive cosmological constant does not go asymptotically to zero for large distances, which is to say that $E < 0$ is not stringent enough to guarantee a bound system. Therefore, we rather rely on the numerical solutions from which, for every n, we infer the value of $\mathcal{A}_n$ such that

$$\rho_c \geqslant \mathcal{A}_n \rho_{\mathrm{vac}}. \tag{28}$$

This gives us the lowest possible central density in terms of ρ_{vac}. The behavior of the ζ_{crit}, the functions f_i, the solution $\xi_1(\zeta_c = \zeta_{\mathrm{crit}}, n)$ and the values of $\mathcal{A}_n$ are shown in fig 2. Note that this inequality can be understood as a generalization of the equilibrium condition $\varrho > \mathcal{A}\rho_{\mathrm{vac}}$, which, when applied for a spherical homogeneous configurations yields $\mathcal{A} = 2$ with $\varrho = \rho =$ constant (Balaguera-Antolínez & Nowakowski 2005; Balaguera-Antolínez,Böhmer & Nowakowski 2005a).

Note that, at $n = 5$ the radius of the configuration becomes undefined, as well as the energy. A $n = 5$ polytrope is highly concentrated at the center (Chandrasekhar 1967). No criteria can be written since even for $\rho_{\mathrm{vac}} = 0$ there is not a finite radius. But it is this high concentration at the center and a smooth asymptotic behavior which makes this case still a viable phenomenological model if Λ is zero. On the contrary for non-zero, positive Λ the solutions start oscillating around $2\rho_{\mathrm{vac}}$ which makes the definition of the radius more problematic. For $n \to \infty$ the polytropic e.o.s describes an ideal gas (isothermal sphere). Since in this limit the expressions derived before are not well definite, this case will be explored in more detail in the next section. In spite of the mathematical differences, the isothermal sphere bears many similarities to the cases $n \geqslant 5$ and our conclusions regarding the definition of a radius in the $n \to \infty$ case equally apply to finite n bigger than 5.

3.2 Effects with generalized dark energy equation of state

In the last section we have explored the effects of a dark energy-dominated background with the equation of state $\omega_{\mathrm{x}} = -1$. Other dark energy models are often used with $\omega_{\mathrm{x}} = -1/3$ and $\omega_{\mathrm{x}} = -2/3$ or even $\omega_{\mathrm{x}} < -1$, in the so-called phantom regime, or even a time dependent dark energy model (quintessence). A simple generalization to such models can be easily done by making the following replacement in our equations

$$\zeta \to \zeta(a)_{\mathrm{eff}} \equiv -\frac{1}{2}\zeta\eta(a)a^{-f(a)}, \tag{29}$$

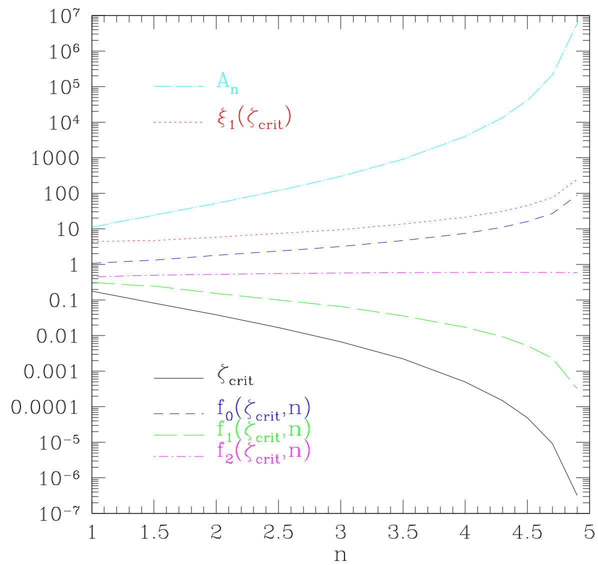

Figure 2. The values of $\zeta_{\rm crit}$, $\xi(\zeta_{\rm crit})$, the functions $f_i(\zeta_{\rm c}; n)$, and $\mathcal{A}_n = 2\zeta_{\rm crit}^{-1}$. Equilibrium configurations are reached for $\rho_{\rm c} > \mathcal{A}_n\rho_{\rm vac}$ (for a ΛCDM cosmoolgy one has to rewrite $\mathcal{A}_n \to 0.81\mathcal{A}_n$).

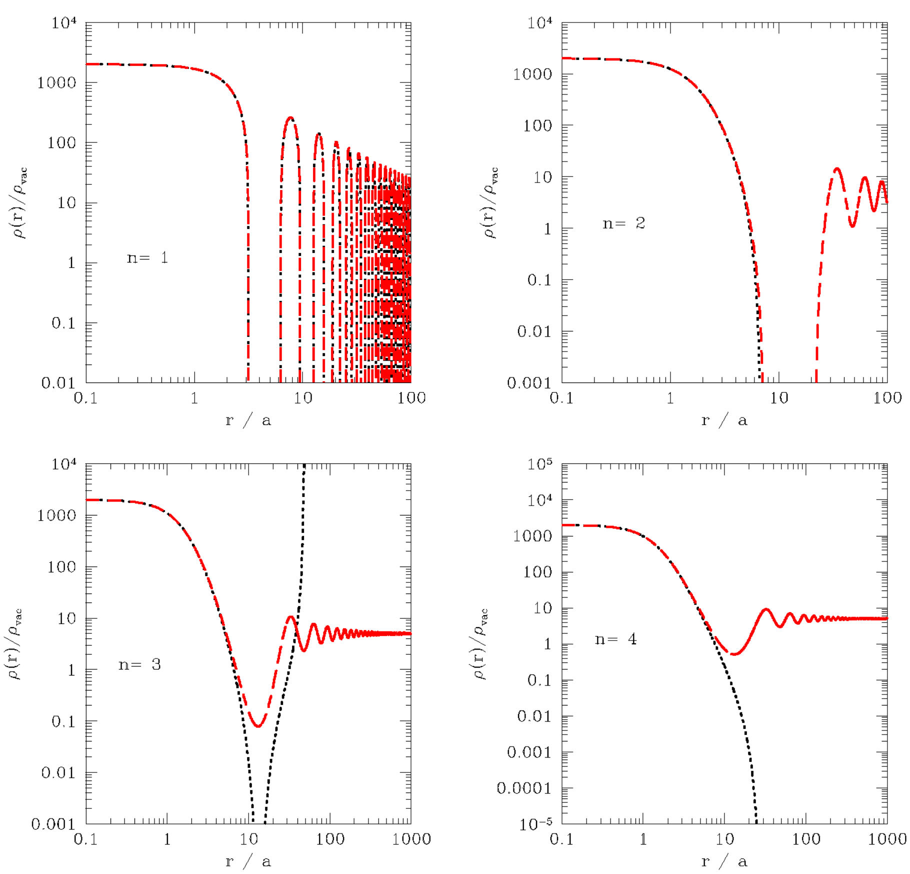

Figure 3. Density of a polytropic configuration for $\zeta_{\rm c} = 10^{-3}$ and different polytropic index in a modified Newton-Hook space time with a dark energy equation of state $\omega_{\rm x} = -2/3$ (black,dots) and $\omega_{\rm x} = -2$ (red,short dash). Compare with Fig.1

where $\eta(a) = 1 + 3\omega_{\rm x}(a)$, and where the function $f(a)$ is defined in Eq.(2). Note that for this generalization to be coherent with the derivation of ΛLE in (17), one needs to consider that the equation of state is close to -1, so that there is almost no time-dependence, and the energy density for dark energy is almost constant. This is indeed the case for most popular candidates of dark energy specially at low redshifts $z < 1$. Also, notice once again, that we are still assuming an homogeneous dark energy component which flows freely to and from the overdensity. Hence, violating energy conservation inside it. Clearly, other models of dark energy will posses dynamical properties that the cosmological constant does not have. For instance, we could allow some fraction of dark energy to take part in the collapse and virialization (Maor & Lahav 2005; Caimmi 2007; Mota & van de Bruck 2004), which would lead to the presence of self and cross interaction terms for dark energy and the (polytropic like) matter in Euler equation, which at the end modifies the Lane Emden equation. With this simplistic approach, we see that the effects with a general equation of state are smaller than those associated to the cosmological constant. In particular, the equation of state $\omega_{\rm x} = -1/3$ displays a null effects since it implies $\eta = 0$ (note that this equation of state can also resemble the curvature term in evolution equation for the background). On the other hand, phantom models of dark energy, which are associated to equations of state $\omega_{\rm x} < -1$(Caldwell 2002; Nojiri 2005), have quite a strong effect. In Fig. 3 we show numerical solutions of Lane-Emden equations for a background dominated with dark energy with $\omega_{\rm x} = -2/3$ and a phantom dark energy with $\omega_{\rm x} = -2$, with $\zeta = 10^{-3}$. These curves are to be compared with those at fig.1. Clearly equations of state with $\omega_{\rm x} < -1$ will generate larger radius than the case described in the main text. Furthermore, the asymptotic behavior of the ratio between the density and $\rho_{\rm vac}$ is $\rho/\rho_{\rm vac} \to |\eta|$.

3.3 Stability criteria with cosmological constant

Stability criteria for polytropic configurations can be derived from the virial equation. Using equations (23), (24) and (25) we can write the virial theorem (10) in terms of the radius R and the mass M:

$$-\frac{M^2}{2R} + \frac{1}{2}(5-n)\kappa\rho_{\rm c}^{\frac{1}{n}} M f_2 + \frac{2}{3}\pi\rho_{\rm vac} M R^2 \left(5f_1 - 1\right) = 0, \tag{30}$$

where we have assumed that the only contribution to the kinetic energy comes from the pressure in the form of $\mathcal{K} = \frac{3}{2}\Pi$. Note that for $\rho_{\rm vac} = 0$ and finite mass, one obtains $R \propto (5-n)^{-1}$ while for $\rho_{\rm vac} \neq 0$ we would obtain a cubic equation for the radius. Instead of solving for the virial radius, we solve for the mass as a function of central density with the help of Eq (21). We have

$$M = \mathcal{G}\rho_{\rm c}^{\frac{3-n}{2n}}, \qquad \mathcal{G} = \mathcal{G}(\zeta_{\rm c}; n) \equiv \left[\frac{\kappa f_0 f_2 (5-n)}{1 - \frac{2}{3}\pi\zeta_{\rm c} f_0^3 (5f_1 - 1)}\right]^{\frac{3}{2}}. \tag{31}$$

The explicit dependence of the mass with respect to the central density splits into two parts: on one hand it has the same form as the usual case with $\Lambda = 0$, that is, $\rho_{\rm c}^{(3-n)/2n}$; on the other hand the function $\mathcal{G}$ has a complicated dependence on the central density because of the term $\zeta_{\rm c}$. With the help of (21) and (31) we can write a mass-radius relation and the radius-central density relation

$$M = \left(\mathcal{G}^{\frac{2}{3}\left(\frac{n}{n-1}\right)} f_0^{\frac{3-n}{n-1}}\right) R^{\frac{3-n}{1-n}}, \qquad R = \left(\mathcal{G}^{\frac{1}{3}} f_0\right) \rho_{\rm c}^{\frac{1}{2}\left(\frac{1-n}{n}\right)}. \tag{32}$$

Following the stability theorem (see for instance in (Weinberg 1972)), the stability criteria can be determined from the variations of the mass in equilibrium with respect to the central density. We derive from Eq. (32):

$$\frac{\partial M}{\partial \rho_{\rm c}} = \left[\frac{3}{2}\left(\gamma - \frac{4}{3}\right)\rho_c^{-1}\mathcal{G} + \frac{\partial \mathcal{G}}{\partial \rho_{\rm c}}\right]\rho_{\rm c}^{\frac{3}{2}\left(\gamma - \frac{4}{3}\right)}. \tag{33}$$

Stability (instability) stands for $\partial M/\partial\rho_{\rm c} > 0$ ($\partial M/\partial\rho_{\rm c} < 0$). This yields a critical value of the polytropic exponent $\gamma_{\rm crit}$ when $\partial M/\partial\rho_{\rm c} = 0$ given by

$$\gamma_{\rm crit} = \gamma_{\rm crit}(\zeta_c) \equiv \frac{4}{3} + \frac{2}{3}\frac{\partial \ln \mathcal{G}}{\partial \ln \rho_{\rm c}}, \tag{34}$$

in the sense that polytropic configurations are stable under small radial perturbations if $\gamma > \gamma_{\rm crit}$. It is clear that the second term in (34) also depends on the polytropic index and therefore this equation is essentially a transcendental expression for $\gamma_{\rm crit}$.

It is worth mentioning that by including the corrections due to general relativity, the critical value for $\gamma_{\rm crit}$ is also modified as $\gamma_{\rm crit} = (4/3) + R_{\rm s}/R$ (Shapiro & Teukolsky 1983) and hence for compact objects the correction to the critical polytropic index is stronger from the effects of general relativity than from the effects of the background. This is as we would expect it. Stability of relativistic configurations with non-zero cosmological constant has been explored in (Böhmer & Harko 2005; Böhmer 2004).

Going back to equation (31), we can write the mass of the configuration as $M = \alpha_M M(0)$, where $M(0)$ is the mass when $\Lambda = 0$ and $\alpha_M = \alpha_M(\zeta_{\rm c}, n)$ is the enhancement factor. Both quantities can be calculated to give

n	$\zeta_c = 0.1$	$\zeta_c = 0.05$	$\zeta_c = 0.001$
1	$(1.12, 1.29)$	$(1.05, 1.12)$	$(1.001, 1.002)$
1.5	$(-,-)$	$(1.11, 1.17$	$(1.002, 1.003)$
3	$(-,-)$	$(-,-)$	$(1.022, 1.01)$

Table 1. Numerical values for the enhancement factors (α_R, α_M) (values for $n = 1$ have been taken from (Balaguera-Antolínez & Nowakowski 2005)). The symbol $-$ indicates a non defined radius.

$$M(0) \equiv \left(\kappa(5-n) f_0^{(n)} f_2^{(n)}\right)^{\frac{3}{2}} \rho_c^{\frac{3-n}{2n}}, \qquad \alpha_M \equiv \left[\frac{f_0 f_2}{f_0^{(n)} f_2^{(n)} \left(1 - \frac{2}{3}\pi\zeta_c f_0^3 (5f_1 - 1)\right)}\right]^{\frac{3}{2}}, \tag{35}$$

where $f_i^{(n)} \equiv f_i(\zeta_c = 0, n)$ are numerical factors (tabulated in table 1) that can be determined in a straightforward way. Similarly, by using Eq (21), the radius can be written as $R = \alpha_R R(0)$, where

$$R(0) = \left(\kappa(5-n) f_0^{(n)} f_2^{(n)}\right)^{\frac{1}{2}} f_0^{(n)} \rho_c^{\frac{1-n}{2n}}, \quad \alpha_R \equiv \left(\frac{f_0}{f_0^{(n)}}\right) \left[\frac{f_0 f_2}{f_0^{(n)} f_2^{(n)} \left(1 - \frac{2}{3}\pi\zeta_c f_0^3 (5f_1 - 1)\right)}\right]^{\frac{1}{2}}. \tag{36}$$

In table 1 we show the values of the enhancement factors α_M and α_R for different values of ζ_c and different polytropic index n. We also show the values of the critical ratio $\zeta_{\rm crit}$ which separates the configurations with definite ratio such that a zero ξ_1 exist provided that $\zeta_c < \zeta_{\rm crit}$. We will show some examples where the enhancement factors may be relevant in section 5.

4 THE ISOTHERMAL SPHERE

The isothermal sphere is a popular model in astrophysics, either to model large astrophysical and cosmological objects (galaxies, galaxy clusters) (Lynden-Bell & Wood 1968; Penston 1969; Yabushita 1968; Sommer-Larsen,Vedel & Hellsten 1996; Chavanis 2001; Sussman & Hernandez 2003), to examine the so-called gravothermal catastrophe (Binney & Tremaine 1987; Natarajan & Lynden-Bell 1997; Lombardi & Berti 2001) and finally to compare observations with model predictions (Rines et al. 2002; Sussman & Hernandez 2003). In the limit $n \to \infty$ in the polytropic equation of state one obtains the description for an isothermal sphere, (ideal gas configuration) with

$$p = \sigma^2 \rho \tag{37}$$

where σ is the velocity dispersion ($\sigma^2 \propto T$). The pattern we found in section 3 for $n \geqslant 5$ gets confirmed here: no finite radius of the configurations is found with Λ, the asymptotic behavior is not $\rho \to 0$ as $r \to \infty$ (but rather $\rho \to 2\rho_{\rm vac}$) and, as we will show below, other attempts to define a proper finite radius are not satisfactory.

The results for a finite value of the index n are defined in the limit $n \to \infty$ only asymptotically in the case $\Lambda = 0$. We consider this as an acceptable behavior of the density. Because of the limiting case $n \to \infty$ the analysis for the isothermal sphere must be done in a slightly different way. As was done in Eq. (13), we can integrate the equilibrium equations (Euler and Poisson's equations) and obtain an explicit dependence of the density with $\rho_{\rm vac}$ as

$$\rho(r) = \rho_c \exp\left[-\frac{1}{\sigma^2}(\Phi_{\rm grav}(r) - \Phi_{\rm grav}(0))\right] \exp\left[\frac{8}{3\sigma^2}\pi\rho_{\rm vac} r^2\right], \tag{38}$$

The resulting differential equation for the density with cosmological constant can be written as

$$\frac{\sigma^2}{r^2}\frac{{\rm d}}{{\rm d}r}\left(r^2 \frac{{\rm d}\ln\rho}{{\rm d}r}\right) = -4\pi\rho + 8\pi\rho_{\rm vac}, \tag{39}$$

This differential equation could be treated in the same way as we did for the polytropic equation of state, i.e, by defining a new function $\psi \sim \rho/\rho_c$, but here we can already use the fact that the cosmological constant introduces scales of density, length and time (Balaguera-Antolínez,Böhmer & Nowakowski 2006b). Let us then define the function $\psi(\xi) = \ln(\rho(r_0\xi)/\rho_{\rm vac})$ and $r = r_0\xi$, with r_0 the associated length scale. Since we are now scaling the density with $\rho_{\rm vac}$, the associated length scale r_0 should be also scaled by the length scale imposed by Λ:

$$r_0 = \sigma r_\Lambda = 13.34 \left(\frac{\sigma}{10^3\ {\rm km/s}}\right) {\rm Mpc}. \tag{40}$$

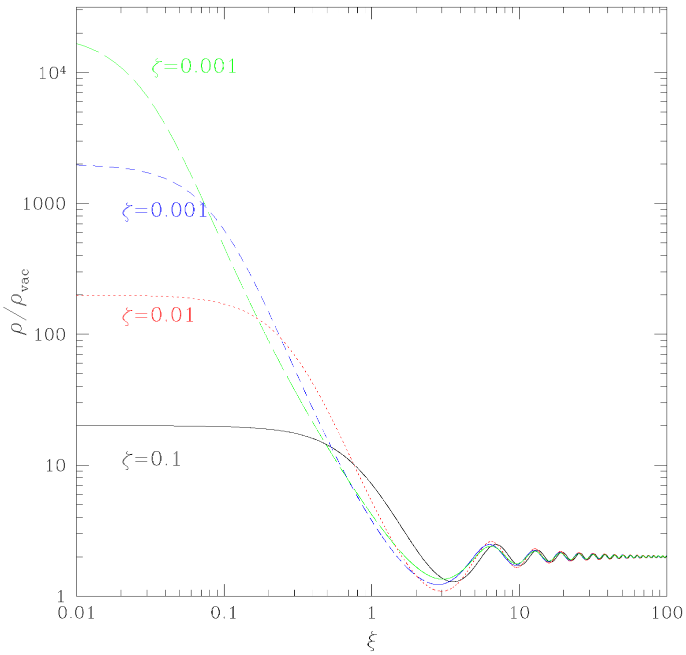

Figure 4. Scaled density $\rho/\rho_{\rm vac} = e^{\psi}$ for the isothermal sphere at different values of central density. The solutions oscillate around the value $\rho = 2\rho_{\rm vac}$.

For an hydrogen cloud with $\sigma \sim 4$ km/s we have $r_0 \approx 40$ kpc which is approximately the radius of an elliptical (E0) galaxy. In terms of the function $\psi(\xi)$, the differential equation governing the density profile is then written as [1]

$$\frac{1}{\xi^2}\frac{\mathrm{d}}{\mathrm{d}\xi}\left(\xi^2\frac{\mathrm{d}\psi}{\mathrm{d}\xi}\right) = 1 - \frac{1}{2}e^{\psi}, \tag{41}$$

so that according to Eq. (38) we may write

$$\psi(r/r_0) = \ln\left(\frac{\rho_{\rm c}}{\rho_{\rm vac}}\right) - \sigma^{-2}\left(\Phi_{\rm grav}(r) - \frac{8}{3}\pi\rho_{\rm vac}r^2\right). \tag{42}$$

From this we can derive different solutions ψ depending on the initial condition $\psi(\xi = 0) = \ln(\rho_{\rm c}/\rho_{\rm vac})$ and $\mathrm{d}\psi(\xi)/\mathrm{d}\xi = 0$ at $\xi = 0$. In Fig. 4 we show numerical results for the solutions of equation (41) using different values values of $\rho_{\rm c}/\rho_{\rm vac}$. As it is the case for $n > 5$, the radius cannot be defined by searching the first zero of the density i.e. the value ξ_1 such that $e^{\psi(\xi_1)} = 0$ (including $\psi \to -\infty$). In this case, the behavior of the derivative of the density profile changes as compared with the the $\Lambda = 0$ case since with increasing ξ the density starts oscillating around the value $\rho = 2\rho_{\rm vac}$ such that for $\xi \to \infty$ one has a solution $\rho \to 2\rho_{\rm vac}$. This can be checked from (41) which corresponds to the first non trivial solution for ρ. This behavior implies that there exist a value of $\xi = \xi_1$ where the derivative changes sign and hence the validity of the physical condition required for any realistic model i.e. $\mathrm{d}\rho/\mathrm{d}r < 0$ should be given up unless we define the size of the configuration as the radius at the value of the first local minimum. We will come back to this option below to show that it is not acceptable. A second option would be to set the radius at the position where the density acquires for the first time its asymptotic value $2\rho_{\rm vac}$. We could motivate such a definition by demanding that the density at the boundary goes smoothly to the background density. This is for tow reasons, however, not justified. First, we recall that a positive cosmological constant leads to a repulsive 'force' as it accelerates the expansion. A negative cosmological constant could be modeled in a Newtonian sense by a constant positive density which, however, is strictly speaking still not a background density. Secondly, if we include the background density ρ_b we would have started with $\rho + \rho_b$ (with a dynamical equation for ρ being ρ_b =constant) in which case the boundary condition would again be $\rho(R) = 0$ to define the extension of the body (or at least, $\rho \to \infty$ as $r \to \infty$). Hence, this second option can be excluded on general grounds. In any case as can be seen from Figure 4 both definitions would yield two different values of radius. Since the first candidate to define a radius is based upon a physical condition of the configuration, we could expect this definition as the more suitable one. However such a definition must be in agreement with the observed values for masses and radius of

[1] Compare with Eq. 374 of (Chandrasekhar 1967) or Eq.1 of (Natarajan & Lynden-Bell 1997) where the density is scaled by the central density. The factor 1 on the r.h.s of (41) is due to $\rho_{\rm vac}$.

R/kpc	ξ_1	$\rho_c/\rho(R)$	$M/M_\odot$	$\bar{\rho}$ (gr/cm^3)
10	0.00249	1.0005	2.17×10^8	3.4×10^{-25}
50	0.01248	1.0129	2.7×10^{10}	1.94×10^{-25}
100	0.0249	1.052	2.11×10^{11}	7.2×10^{-26}

Table 2. Values for ξ_1, $\rho_c/\rho(R)$ and the mass for different values of radius and for $\rho_c = 10^3\rho_{\rm vac}$ with $\sigma = 300$km/s.

specific configurations and the validity of this definition can be put to test by the total mass of the configuration, given as

$$M = 1.55 \times 10^{15}\left(\frac{\sigma}{10^3\,{\rm km/s}}\right)^3 f(\xi_1)\,M_\odot, \qquad f(\xi_1) \equiv \int_0^{\xi_1}\xi^2 e^{\psi}{\rm d}\xi. \tag{43}$$

Combining (40) and (43) we can write

$$M = 653.55\left(\frac{R}{\rm kpc}\right)^3 \xi_1^{-3} f(\xi_1)\,M_\odot. \tag{44}$$

If we define the radius at the first minimum (see Fig. 4), we find $M \approx 2\times10^9\,(R/{\rm kpc})^3\,M_\odot$. Although this might set the right order of magnitude for the mass of a E0 galaxy if we insist on realistic values for the respective radius, say $R \sim 10$ kpc, the picture changes again as the radius is fixed by (40) which gives $R \approx 5.3\times10^6\,\big(\sigma/10^3{\rm km/s}\big)$ kpc. In order to get a radius of the order of kpc with masses of the order of $10^{10}M_\odot$ we would require $\sigma \sim 10^{-5}$km/s. This differs by almost eight orders of magnitude with the measured values for the velocity dispersion σ in elliptical galaxies ($\sigma \sim 300$ km/s) or with the Faber-Jackson Law for velocity dispersion (Padmananbhan 1993). We conclude that defining the radius by the position of the first minimum is not a realistic solution. As the last option to get realistic values for the parameters of the configuration we consider the brute force method to simply fix the value of ξ_1. It is understood, however, that this method is not acceptable if we insist that the model under consideration has some appealing features (without such features almost any model would be phenomenologically viable). Therefore we discuss this option only for completeness. For a configuration with $\rho_c = 10^5\rho_{\rm vac}$, say an elliptical galaxy, we fix the radius at $R \sim 50$ kpc in Eq.(40) and using a typical value for the velocity dispersion $\sigma \sim 300$ km/s we get $\xi_1 \sim 0.012$ which implies $f(\xi_1) \sim 0.036$. The mass in Eq.(43) is then given as $M \sim 1.5\times10^{12}M_\odot$ while the density at the boundary is $\rho_R \sim 36000\rho_{\rm vac}$, that is, $\rho_c \sim 2.35\rho_R$. In table 2 we perform the same exercise for other radii. The resulting mean density is in accordance with the observed values of the mean density of astrophysical objects ranging from an small elliptical galaxy to a galaxy cluster. However, as mentioned above, the model introduces an arbitrary cut-off and cannot be considered as a consistent model of hydrostatic equilibrium.

In summary, the attempts to define a finite radius for the isothermal sphere fail in the presence of a cosmological constant either because such a model fails to reproduce certain phenomenological values (if the definition of the radius is fixed by the first minimum) or because the definition is technically speaking quite artificial to the extent of introducing arbitrary cut-offs. Note that this conclusion is valid almost for any object as the density of the isothermal sphere with Λ has a minimum whatever the central density we choose.

5 EXOTIC ASTROPHYSICAL CONFIGURATIONS

In this section we will probe into the possibilities of exotic, low density configurations. The global interest in such structures is twofold. First, the cosmological constant will affect the properties of low density objects. Secondly, Λ plays effectively the role of an external, repulsive force. Hence a relevant issue that arises in this context is to see whether the vacuum energy density can partly *replace* the pressure which essentially is encoded in the parameter κ ($p = \kappa\rho^\gamma$). By the word *replace* we mean that we want to explore the possibility of a finite radius as long as the pressure effects are small in the presence of $\rho_{\rm vac}$.

5.1 Minimal density configurations

As mentioned above the effect of a positive cosmological constant on matter is best understood as an external repulsive force. In previous sections we have probed into one extreme which describes the situation where a relatively low density object is pulled apart by this force (to an extent that we concluded that the isothermal sphere is not a viable model in the presence of Λ). Limiting conditions when this happens were derived. On the other hand, approaching with our parameters these limiting conditions, but remaining still on the side of equilibrium, means that relatively low density objects can be still in equilibrium thanks to the positive cosmological constant. The best way to investigate low density structures is to to use the lowest possible central density. As explained in section 3, for every n there exist a $\mathcal{A}_n$ such that $\rho_c \geqslant \mathcal{A}_n\rho_{\rm vac}$ which defines the lowest central density. Certainly, a question of interest is to see what such objects would look like. We start with the parameters of the

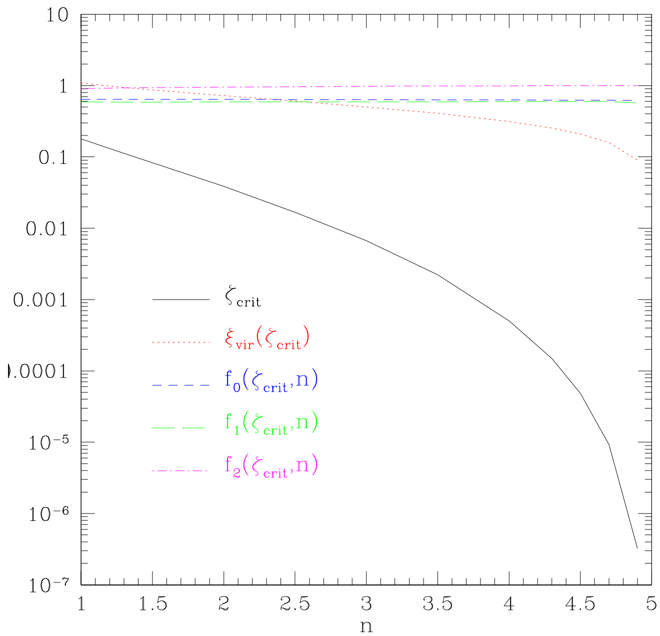

Figure 5. Same as fig. 2, now the functions f_i being evaluated at the value $\xi_{\rm vir}$ solution of Eq.(46).

configuration. The radius at the critical value $\zeta_{\rm crit}$ is given by Eq.(21) after taking the limit $\rho_{\rm c} \rightarrow \mathcal{A}_n \rho_{\rm vac}$ (see (28)). It is given by

$$R_{\rm crit} = 2.175 \left(\frac{M}{10^{12} M_{\odot}} \right)^{1/3} f_0(\zeta_{\rm crit}; n) \zeta_{\rm crit}^{-1/3} \ {\rm Mpc}. \tag{45}$$

From fig. 5 we can see that the product $f_0^3(\zeta_{\rm crit}; n)\zeta_{\rm crit}$ changes a little round the value ~ 0.2 as we change the index n, so that these polytropic configurations will have roughly the same radius (for a given mass). This implies that such configurations have approximately the same average density $\bar{\rho}(\zeta_{\rm crit}) = 1.64\rho_{\rm crit} \approx 2.34\rho_{\rm vac}$. That is, such configurations have a mean density of the order of the of the critical density of the universe. Given such a density we would, at the first glance, suspect that the object described by this density cannot be in equilibrium. However, our result follows strictly from hydrostatic equilibrium and therefore there is no doubt that such object can theoretically exist. Furthermore, $\bar{\rho}$ satisfies the inequalities derived in (Nowakowski & Sanabria & Garcia 2002) and (Balaguera-Antolínez,Böhmer & Nowakowski 2005a) from virial equations and Buchdahl inequalities which guarantee that the object is in equilibrium ($\bar{\rho} > 2\rho_{\rm vac}$). Interestingly, the central density for such objects has to be much higher than $\bar{\rho}$ as, e.g., for $n = 3$ we have $A_3 \approx 300$ and therefore $\rho_{\rm c} > 300\rho_{\rm vac}$. Note that these values have been given from the solution of the Lane-Emden equation, which is a consequence of dynamical equations reduced to describe our system in a steady state. However, we have not tried to solve explicitly quantities from the virial theorem. This makes sense as for Dark Matter Halos (DMH) the parametrized density profiles go often only asymptotically to zero and the radius of DMH is defined as a virial radius where the density is approximately two hundred times over the critical one. Therefore, an analysis using virial equations seems to be adequate here. For constant density Eq.(30) can be expressed as a cubic equation (Balaguera-Antolínez,Böhmer & Nowakowski 2006b) for the radius at which the virial theorem is satisfied (let us ignore for these analysis any surface terms coming from the tensor virial equation). However, if the density is not constant, this expression becomes a transcendental equation for the dimensionless radius $\xi_{\rm vir} = R_{\rm vir}/a$. This equation is

$$\xi_{\rm vir}^2 = \frac{6(5-n)f_0^3}{(n+1)\left[3 - 2\pi\zeta_{\rm c}(5f_1 - 1)f_0^3\right]}, \tag{46}$$

understanding the functions f_i now as integrals up to the value $\xi_{\rm vir}$. Once we fix $\zeta_{\rm crit}$ for a given index n, we use as a first guess for the iteration process the value $\xi_1(\zeta_{\rm crit})$. In fig 5 we show the behavior of the functions f_i and the solutions of Eq.(46). For these values, Eq. (45) gives for $n = 3$ a radius

$$R_{\rm vir} = 25.8 \left(\frac{M}{M_{\odot}} \right)^{1/3} \ {\rm pc}, \tag{47}$$

which can be compared with the radius-mass relation derived in the top-hat sphericall collapse (Padmananbhan 1993)

$$R_{\rm vir} = 21.5h^{-2/3}(1+z_{\rm vir})^{-1}\left(\frac{M}{M_\odot}\right)^{1/3}\ \text{pc}, \tag{48}$$

where h is the dimensionless Hubble parameter and $z_{\rm vir}$ is the redshift of virialization. The resulting average density is then of the order of the value predicted by the top-hat sphericall model:

$$\bar{\rho} = \left(\frac{3\Omega_{\rm vac}}{2\pi\zeta_{\rm crit}f_0^3}\right)\rho_{\rm crit} \approx 200\rho_{\rm crit}, \tag{49}$$

Note with the help of Eq.(16) and (45) that the mass can be written as proportional to the parameter $\kappa^{3/2}$ (introduced in the polytropic equation of state Eq.(11)). Therefore $\kappa \to 0$ is equivalent to choosing a small pressure and, at the same time, a small mass which, in case of a relatively small radius, amounts to a diluted configuration with small density and pressure. Without Λ such configurations would be hardly in equilibrium. Hence, for the configuration which has the extension of pc, Eq.(47), with one solar mass we conclude that the equilibrium is not fully due to the pressure, but partially maintained also by Λ. This is possible, as Λ exerts an outwardly directed non local force on the body. Other mean densities, also independent of M are for $n = 1.5$ and $n = 4$, respectively:

$$\bar{\rho} = 15.3\rho_{\rm crit}, \qquad \bar{\rho} = 2.6\times 10^3\rho_{\rm crit}, \tag{50}$$

The first value is close to $\rho_{\rm crit}$ and therefore also to $\rho_{\rm vac}$. Certainly, if in this example we choose a small mass, equivalent to choosing a negligible pressure, part of the equilibrium is maintained by the repulsive force of Λ. In (Balaguera-Antolínez,Böhmer & Nowakowski we found a simple solution of the hydrostatic equation which has a constant density of the order of $\rho_{\rm vac}$. The above is a non-constant and non-trivial generalization of this solution.

5.2 Cold white dwarfs

The neutrino stars which we will discuss in the subsequent subsection are modeled in close analogy to white dwarfs. Therefore it makes sense to recall some part of the physics of white dwarfs. In addition we can contrast the example of white dwarfs to the low density cases affected by Λ.

In the limit where the thermal energy $k_{\rm B}T$ of a (Newtonian) white dwarf is much smaller than the energy at rest of the electrons (p_F, these configurations can be treated as polytropic configuration with $n = 3$. This is the ultra-relativistic limit where the mass of electrons is much smaller than Fermi's momentum $p_{\rm F}$. In the opposite case we obtain a polytrope or configuration with $n = 3/2$. (Weinberg 1972; Shapiro & Teukolsky 1983). In both cases, the parameter κ_n from the polytropic equation of state is given as

$$\kappa_3 = \frac{1}{12\pi^2}\left(\frac{3\pi^2}{m_n\mu}\right)^{\frac{4}{3}}, \qquad \kappa_{3/2} = \frac{1}{15m_e\pi^2}\left(\frac{3\pi^2}{m_n\mu}\right)^{\frac{5}{3}}, \tag{51}$$

where m_n is the nucleon mass, m_e is the electron mass and μ is the number of nucleons per electron. Using the Newtonian limit with cosmological constant, we can derive the mass and radius of these configurations in equilibrium. In the first case, for $n = 3$ the mass is written using (31) as $M_0 = \mathcal{G}(n = 3)$ which corresponds approximately to the Chandrasekhar's limit (strictly speaking a configuration would have the critical mass, i.e, the Chandrasekhar's limit, if its polytropic index γ is such that $\gamma = \gamma_{\rm crit}$). For this situation one has $M_0(n = 3) = 5.87\mu^{-2}M_\odot$ and $R_0(n = 3) = 6.8(\bar{\rho}_\odot/\rho_{\rm c})^{1/3}\mu^{-\frac{2}{3}}R_\odot$. On the other hand, for $n = 3/2$ one obtains $M_0(n = 3/2) = 3.3\times 10^{-3}(\bar{\rho}_\odot/\rho_{\rm c})^{-1/2}\mu^{-5/2}M_\odot$ and the radius is given by $R_0(n = 3/2) = 0.27(\bar{\rho}_\odot/\rho_{\rm c})^{1/6}\mu^{-\frac{5}{6}}R_\odot$ where $\bar{\rho}_\odot$ is the mean density of the sun. Since for these configurations the ratio $\zeta_{\rm c}$ is much smaller than 10^{-4} we see from Fig. 2 that the effects of Λ are almost negligible. The critical value of the ratio $\zeta_{\rm c}$ gives for $n = 3$ the inequality $\rho_{\rm c} > 307.69\rho_{\rm vac}$ and for $n = 3/2$ the same limit reads $\rho_{\rm c} > 24.24\rho_{\rm vac}$. Central densities of white dwarfs are of the order of $10^5\,\text{gr/cm}^3$ which corresponds to a deviation of nearly thirty orders of magnitude of $\rho_{\rm vac}$.

5.3 Neutrino stars

An interesting possibility is to determine the effects of $\rho_{\rm vac}$ on configurations formed by light fermions. Such configurations can be used, for instance, to model galactic halos (Dolgov & Hansen 2002; Lattanzi,Ruffini & Vereshchagin 2003; Jetzer 1996; Börner 2004). While discussing the phenomenological interest of fermion stars below, we intend to describe such a halo. Clearly, these kind of systems will maintain equilibrium by counterbalancing gravity with the degeneracy pressure as in a white dwarf. For stable configurations, i.e, $n = 3/2$, one must replace the mass of the electron and nucleon by the mass of the considered fermion and set $\mu = 1$ in (51) and (31). We then get for the mass and the radius:

$$M_0 \;=\; 3.28\times 10^{28}\left(\frac{\rho_c}{\bar{\rho}_\odot}\right)^{\frac{1}{2}}\left(\frac{\rm eV}{m_f}\right)^4 M_\odot \;=\; 3.64\times 10^{14}\zeta_{\rm c}^{-1/2}\left(\frac{\rm eV}{m_f}\right)^4 M_\odot, \tag{52}$$

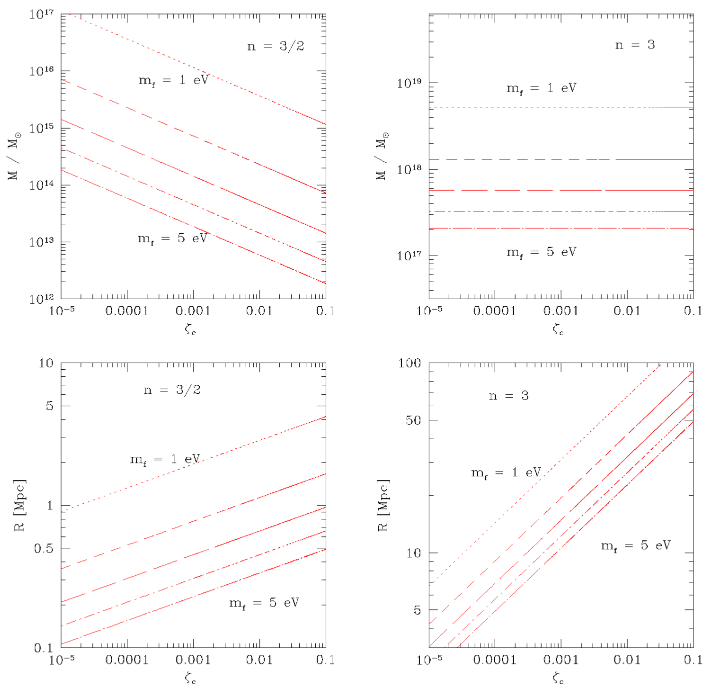

Figure 6. Mass and radius for different central densities, for index $n = 3$ and $n = 3/2$. The masses range from $m_f = 1$ eV up to $m_f = 5$ eV.

$$R_0 = 1.31 \times 10^{-4} \left(\frac{\rho_c}{\bar{\rho}_\odot}\right)^{-\frac{1}{6}} \left(\frac{\mathrm{eV}}{m_f}\right)^{\frac{4}{3}} \mathrm{Mpc} = 6.16\zeta_c^{1/6} \left(\frac{\mathrm{eV}}{m_f}\right)^{\frac{4}{3}} \mathrm{Mpc}.$$

On the other hand, for $n = 3$ one has

$$M_0 = 5.16 \times 10^{18} \left(\frac{\mathrm{eV}}{m_f}\right)^2 M_\odot, \tag{53}$$

$$R_0 = 0.14 \left(\frac{\mathrm{eV}}{m_f}\right)^{\frac{2}{3}} \left(\frac{\rho_c}{\bar{\rho}_\odot}\right)^{-\frac{1}{3}} \mathrm{pc} = 3.1 \times 10^5 \zeta_c^{1/3} \left(\frac{\mathrm{eV}}{m_\mathrm{f}}\right)^{2/3} \mathrm{pc},$$

The cases represent, among other, possible cosmological configurations when the fermion mass if of the order of eV, for instance, massive neutrinos. In figure 6 some representative values for the choice $m_f = 1$ eV up to $m_f = 5$ eV are given. Obviously in the case $n = 1.5$ the values for the mass and radius are sensitive to the choice of m_f. Indeed, the dependence on the fermion mass is much stronger than on the central density. It is justified to speculate that a relative low density objects, affected by Λ, might exist. If then, as in an example we choose $m_f \sim 5$ eV and $\rho_c \sim 40\rho_{\mathrm{vac}}$ then the mass comes out as 10^{12} solar masses with a radius of the order of magnitude of half Mpc which might indeed be the dark matter halo of a galaxy (or at least part of the halo). As pointed out before, such configurations must have a central density greater than $24.4\rho_{\mathrm{vac}}$ in order to be in equilibrium. From table 1 we see that the effect on a configuration with $\zeta_c \sim 0.05$ is represented in an increase in the mass by 17% with respect to M_0 and an increment of 11% in the radius. Then the conclusion would be that Λ affects such a dark matter halo. This is to be taken with some caution as the fermions in such a configuration would be essentially non-relativistic. Note also that it is not clear if neutrinos make up a large fraction of the halo, however, we can also speculate about a low density clustering around luminous matter. Of course, allowing larger central density might change the picture. However, the emerging scenario would not necessarily be a viable phenomenological model. For instance, changing the value of m_f from eV to keV (MeV) would reduce the mass by twelve (twenty four) orders of magnitude which is definitely too small to be of interest. We could counterbalance this by increasing the central density by twenty four (forty eight!) orders of magnitude. Such a 'countermeasure' would, however, result in a reduction of the radius by eight (sixteen!) orders of magnitude, again a too small length scale to be of importance for dark matter halos. In other words, the example with a fermion mass of the order of one eV and low central density is certainly of some phenomenological interest.

The case $n = 3$ is similarly stringent. A neutrino mass of $1 - 5$ eV gives a mass for the entire object of the order of ten to the eighteen solar masses which is too large. A fermion mass of several keV would be suitable for a galaxy halo (a mass of

the order Me V and higher would give a too small total mass). With a relative low central density as before (see Figure 6) we then obtain the right order of magnitude for the halo. But then we will have to live with the fact that such halo reaches up to the next large galaxy. Briefly, we touch upon the other possible application of fermions stars which have been discussed as candidates for the central object in our galaxy. If we allow the extension of this object to be 120 AU and the mass roughly 2.6 million solar masses, then the fermion mass would come out as 10^4 eV for $n = 1.5$ (10^6 eV for $n = 3$) and the central density as $10^{22}\rho_{\rm vac}$ ($10^{28}\rho_{\rm vac}$ for $n = 3$).

5.4 Boson stars

We end the section by putting forward a speculative question in connection with boson stars. The latter are general relativistic geons and can be treated exactly only in general relativistic framework i.e. these kind of configurations are based on the interaction of a massive scalar field and gravitation which leads to gravitational bounded systems. These objects have been also widely discussed as candidates for dark matter (Ruffini & Bonazzola 1969; Lai 2004). On the other hand, variational methods in the connection with the Thomas-Fermi equations give relatively good results even without invoking the whole general relativistic formalism. By including Λ we essentially introduce into the theory a new scale, say in this case a length scale $r_\Lambda = 1/\sqrt{\Lambda}$. The basic parameters of dimension length in a theory with a boson mass m_B and a total mass $M = N_B m_B$ where N_B is the number of bosons are (for a better distinction of the different length scales, we restore in this subsection the value of G_N)

$$L_1 = r_s = G_N M,\ L_2 = r_B = \frac{1}{m_B},\ L_3 = r_\Lambda = \frac{1}{\sqrt{\Lambda}}. \tag{54}$$

The resulting radius of the object's extension can be a combination of these scales i.e.

$$\begin{aligned} R_i^{(1)} &\propto L_i,\ R_i^{(2)} \propto N_B^n L_i \\ R_1 &\propto (L_i^2 L_j)^{1/3},\ R_2 \propto N_B^n R_1 \end{aligned} \tag{55}$$

and similar combination of higher order. Which one of the combination gets chosen, depends on the details of the model. In a close analogy to (Spruch 1991; Eckehard & Schunck 1998) we can examine this taking into account the presence of a positive cosmological constant by considering the energy of such configuration as a two variable function of the mass and the radius $E = E(R, M)$

$$E \sim \frac{N_{\rm B}}{R} - \frac{G_{\rm N} m_{\rm B}^2 N_{\rm B}^2}{R} + \frac{8}{3}\pi G_{\rm N}\rho_{\rm vac} m_{\rm B} N_{\rm B} R^2 \tag{56}$$

The first term corresponds to the total kinetic energy written as $\mathcal{K} = N_{\rm B} p = N_{\rm B}/\lambda$ and taking $\lambda \sim R$. The second term is the gravitational potential energy and the third term corresponds to the contribution of the background (see Eq. (8)). By treating mass and radius as independent variables (we think this this is the right procedure since the radius will depend on the 'external force' due to $\rho_{\rm vac}$), we extremize the energy leading to the following values of mass and radius:

$$M \sim \frac{1}{G_{\rm N} m_{\rm B}} \sim 10^{-10}\left(\frac{\rm eV}{m_{\rm B}}\right) M_\odot, \qquad R \sim \left(\frac{1}{8\pi G_N m_{\rm B}\rho_{\rm vac}}\right)^{1/3} \sim 10^5 \left(\frac{\rm eV}{m_{\rm B}}\right)^{\frac{1}{3}} R_\odot \tag{57}$$

Such values would lead to a mean density of the order of $\bar{\rho} \sim 6\rho_{\rm vac}$ i.e. an extremely low density configuration. The mass given in the last expression is the so-called Kaup limit (Spruch 1991). Of course, this relative simple treatment does not guarantee that the full, general relativistic treatment, will give the same results. Therefore we consider it as a conjecture. However, it is also obvious from the the discussion above that low density boson stars are a real possibility worth pursuing with more rigor (we intend to do so in the near future).

5.5 A comparison between ΛLE profiles and Dark Matter Halos profiles

It is of some importance to see whether our results from the examination of polytropic hydrostatic equilibrium or from the virial equations can be applied to Dark matter configurations. N-body simulations based in a ΛCDM model of the universe show that the density profile of virialized Dark Matter Halos (DMH) can be described by a profile of the form (Navarro & Frenk & White 1996)

$$\rho(r) = (2)^{3-m}\rho_s (r/r_s)^{-m}\left(1 + r/r_s\right)^{m-3}, \tag{58}$$

where r_s is the characteristic radius (the logarithmic slope is $\mathrm{d}\ln\rho/\mathrm{d}\ln r_s = -m + \frac{1}{2}(m-3)$), $\rho_s = \rho(r_s)$ and the index m characterizes the slope of the profile in the central regions of the halo. The mass of the configuration enclosed in the virial radius $r_{\rm vir}$ is given as $M_{\rm vir} = 4\pi(2)^{3-m}\rho_s r_s^3 F(c)$ such that one can write $\rho_s = (1/3)(2)^{m-3}\Delta_{\rm vir}\rho_{\rm crit}c^3 F^{-1}(c)$, where $c = r_{\rm vir}/r_s$ is the concentration parameter, $\Delta_{\rm vir}$ is the ratio between the mean density at the time of virialization and the critical density of the

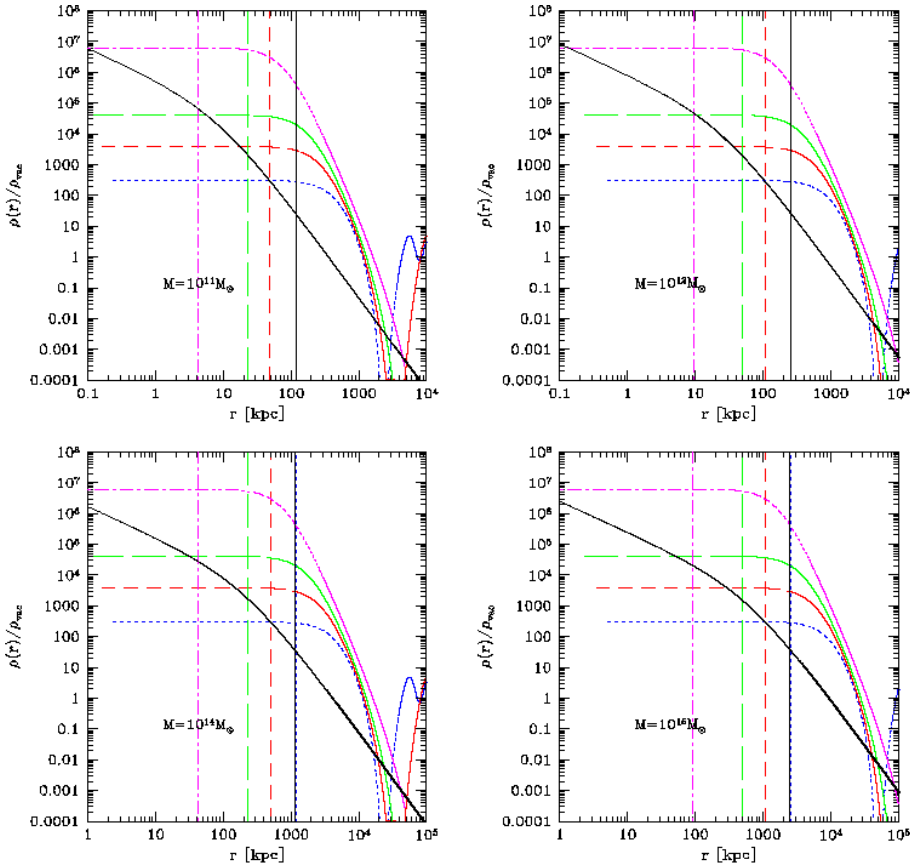

Figure 7. NFW profile (black, solid line) compared to the solutions of ΛLE equation for different masses and different index n ranging from $n = 3$(blue,dots), $n = 4$ (red,short-dashed line), $n = 4.5$ (green,long-dashed line) and $n = 4.9$ (magenta,dot short-dashed line), in the limiting case $\zeta_{\rm c} = \zeta_{\rm crit}$. The solution from LE equation is written for the critical value of the parameter $\zeta_{\rm crit}$, shown in table 2. The vertical black line represents the virial radius from the NFW profile. The vertical colored lines represent the virial radius $R_{\rm vir}(\zeta_{\rm crit}) = a\xi_{\rm vir}$ for the different polytropic indices.

universe ($\Delta_{\rm vir} \approx 18\pi^2$ in the top-hat model for a flat Einstein-deSitter universe, while $\Delta_{\rm vir} \sim 104$ in the ΛCDM cosmological model (Diemand et al 2007)) and $F(c) = \int_0^c x^{2-m}(1+x)^{m-3}{\rm d}x$. This *universal profile* has been widely used in modeling DMH in galaxy clusters, and the comparison of these models with a stellar polytropic-like profile -without the explicit contribution from the cosmological constant in the Lane-Emden equation- can be found in (Cabral-Roseti et al 2004; Arieli 2003).

Some differences can be described between the ΛLE and the NFW profiles. First, on fundamental grounds, it is clear that the NFW profile does not satisfy the LE equation; a basic reason for this is that dark matter is assumed to be collisionless and is only affected by gravity. However, the fact that the real nature of dark matter is still an unsolved issue leaves an open door through which one can introduce interaction between dark matter particles leading to a different equation of state (see for instance (Ren et al. 2006)). On functional forms, one sees that at the central region the difference is abrupt, since the Lane-Emden equation has a flat density profile at $r = 0$, while the NFW profile has a cuspy profile of the form $\rho \sim r^{-m}$. It has been widely discussed how such cuspy profile is inconsistent with data showing central regions of clusters with homogeneous cores (see discussion at the end of this section). Such small slope in the inner regions can be reproduced by the *universal profile* for the case $m = 0$, and for the profile derived from the ΛLE equation (which is just a consequence of initial conditions, and hence, its independent of Λ). In this case, the effects of the cosmological constant can be reduced to explore the outer regions of the halos and compare, for instance, the slope of the profiles and the virial radius predicted by each one.

The density profiles predicted by the ΛLE equation and the NFW profile (for $m = 1$) are presented in fig.7 for the virial radius given by $\xi_{\rm vir}$ and in fig.8 for the radius given by ξ_1, both with $\zeta_{\rm c} = \zeta_{\rm crit}$. Also, the behavior of the radius for different values of mass and polytropic indices are given in Fig 9 (with $r_s \approx 25.3\left(M_{\rm vir}/10^{12}M_{\odot}\right)^{0.46}$ kpc and $r_{\rm vir} = 1.498\Delta_{\rm vir}^{-1/3}\left(M_{\rm vir}/10^{12}M_{\odot}\right)^{1/3}$ Mpc $\approx 255\left(M_{\rm vir}/10^{12}M_{\odot}\right)^{1/3}$ kpc (Gentile & Tonini & Salucci 2007)).

We see that the virial radius given by the ΛLE equation is surprisingly close to the virial radius given by the NFW profile for $n = 3$ in the range of masses shown in fig 9, and as pointed in Eq.(49), this value yields for this model $\Delta_{\rm vir}^{\Lambda LE} \approx 200$. However, as can be seen from the plots, the ΛLE density profile is almost flat until the virial radius. On the other hand, the

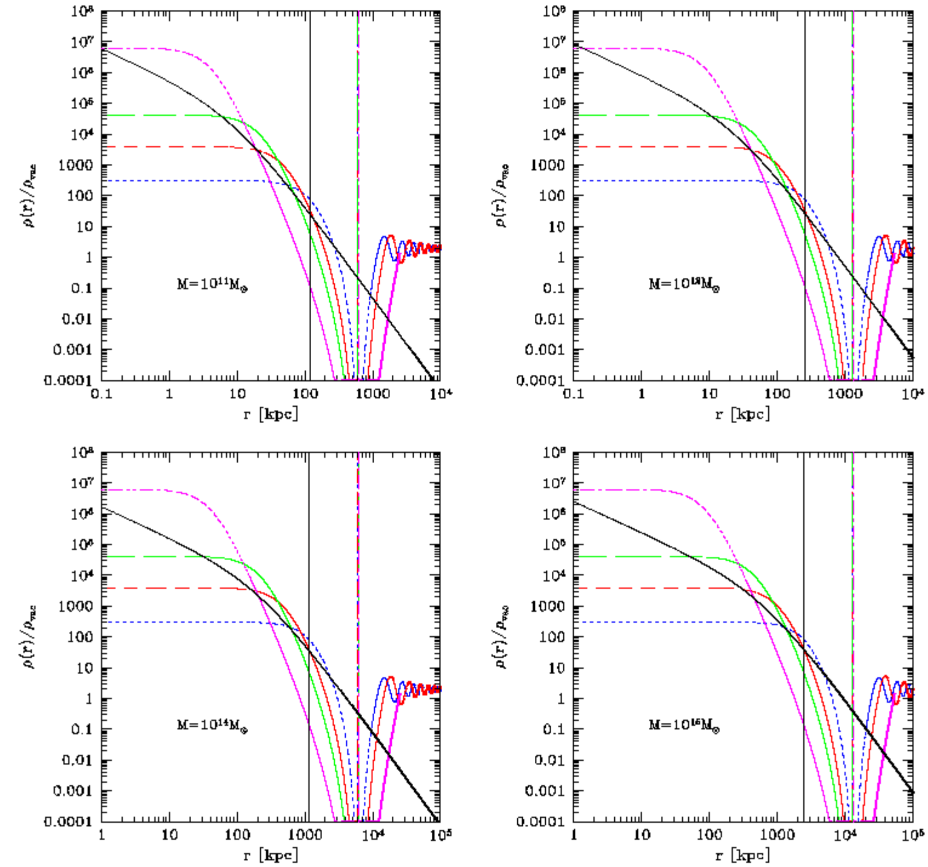

Figure 8. Same as fig 7 but for the radius given by the condition $\psi(\xi_1) = 0$.

$m = 0$ profile allow us to parameterize it as $\rho(r)/\rho_{\rm vac} = 2\zeta_{\rm c}^{-1}(1+r/r_s)^{-3}$, where the concentration parameter c can be written as $c+1 \approx 1.11\zeta_{\rm c}^{1/3}\Delta_{\rm vir}^{1/3}$.

In fig.10 and 11 we have compared both profiles with the corresponding $\zeta_{\rm crit}$ for polytropic index $n = 3$ and $n = 4.9$. For the first case we see that the virial radius are of the same order of magnitude than the one predicted by the NFW profile. For $n = 4.9$, these quantities differ by one order of magnitude. In all cases, the slope of the NFW profiles changes faster than the ΛLE profile, which implies that the polytropic configurations enclosed by $r_{\rm vir}$ display almost a constant density.

The comparison we made above between the polytropic configuration and the NFW profiles shows that up to the cuspy behaviour the polytropic results agree with NFW for the polytropic index $n = 3$. It is worth pointing out here that it is exactly this cuspy behaviour which seems to be at odds with observational facts (Arieli 2003; Matos et al. 2005; Hoeft & Müecket $ Gottlöber 2004). Our result for $n = 3$ is then a good candidate to describe DMH. Indeed, the undesired feature of the cuspy behaviour led at least some groups to model the DMH as a polytropic configuration (Arieli 2003; Dehnen & Rose 1993; Matos et al. 2005; McKee 2001; Debattista & Sellwood 1998; Gonzalez-Casado et al. 2004; Yepes et al. 2004); Henriksen 2004; Hogan & Dalcanton 2000). Sometimes it is claimed that a polytropic model is favoured over the results from N-body simulation (Zavala et al. 2006). However, the oscillatory behavior of the $n = 3$ solutions of the ΛLE represents a disadvantage when compared with the NFW profiles, although the region of physical interest (below the virial radius) is well represented by the solutions of ΛLE.

6 CONCLUSIONS

In this paper we have explored the effects of a positive cosmological constant on the equilibrium and stability of astrophysical configurations with a polytropic equation of state. We have found that the radius of these kind of configurations is affected in the sense that not all polytropic indices yield configurations with definite radius even in the asymptotic sense. Among other, the widely used isothermal sphere model becomes a non-viable model in the presence of Λ unless we are ready to introduce an arbitrary cut-off which renders the model unappealing. Indeed, in this particular case we have tried different definitions of a finite radius with the result that none of them seems to be justified, either from the phenomenological or from the theoretical

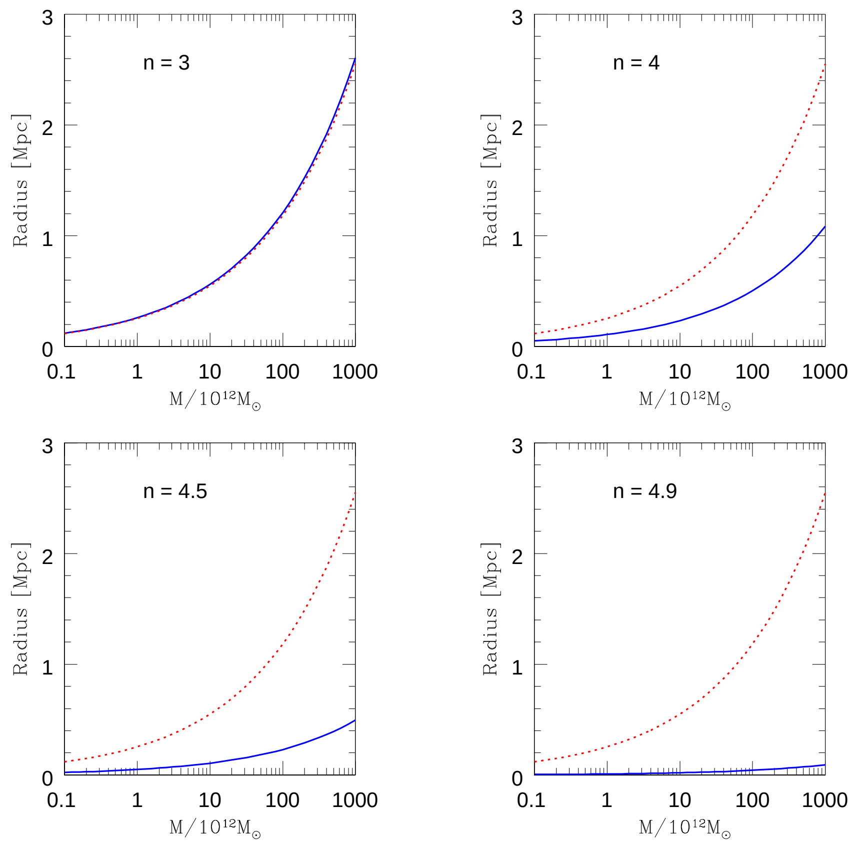

Figure 9. Mass-radius relation for the NFW (red, dashed line) profile compared with the solutions Eq. 46 (blus, solid line) for four different values of n.

point of view. This is then an interesting global result: Λ not only affects quantitatively certain properties of large, low-density astrophysical structures, but it also excludes certain commonly used models regardless what density we use.

For polytropic indexes $n < 5$ and for *certain values* of the central density we cannot find a well definite radius. These *certain values* are encoded in a generalization of the equilibrium condition found for spherical configurations (i.e, $\rho > 2\rho_{\rm vac}$) written now as $\rho_{\rm c} > \mathcal{A}_n\rho_{\rm vac}$. We obtain $\mathcal{A}_1 = 10.8$, $\mathcal{A}_{3/2} = 24.2$, $\mathcal{A}_3 = 307.7$, $\mathcal{A}_4 \approx 4000$. These values set a minimal central density for a given polytropic index n. We have discussed such minimal density configurations and determined their average density which strongly depend on n. Interestingly, the radius of such configurations has a connection to the length scale which appears in the Schwarzschild- de Sitter as the maximally possible radius for bound orbits (Balaguera-Antolínez,Böhmer & Nowakowski 2006b). In this framework we found also a solution of very low, non-constant density. Indeed, the limiting value of the central density in the above equations is a crucial point. Below this value no matter can be in equilibrium. However, above this value low density objects can still exist. Both effects are due to Λ: in the first case the external repulsive force is too strong for the matter to be in equilibrium, in the second case this force can counterbalance the attractive Newtonian gravity effects (even if the pressure is small).

Other examples of low density configuration which we examined in some detail are neutrino stars with mass of the order 1 eV and 1 keV. In there we found that a nowadays dominating cosmological constant affects both the mass as well as the radius of such exotic objects. Such effect could change those physical quantities several orders of magnitude. The magnitude of such effects, however, depend on the fermionic masses and on the assumption that the fermions in such a configuration would be essentially non-relativistic.

Finally, we made a conjecture regarding boson stars, and used variational methods in connection with the Thomas-Fermi equations which could give relatively good results even without invoking the whole general relativistic formalism, We then found extremely low density configurations for such astrophysical objects. Notice however, that this conjecture relied purely on arguments based on scales and in fact needs a full general relativistic investigation to confirm the results here obtained.

We have compared polytropic configurations with Dark Matter density profiles from N-body simulations. Surprisingly,

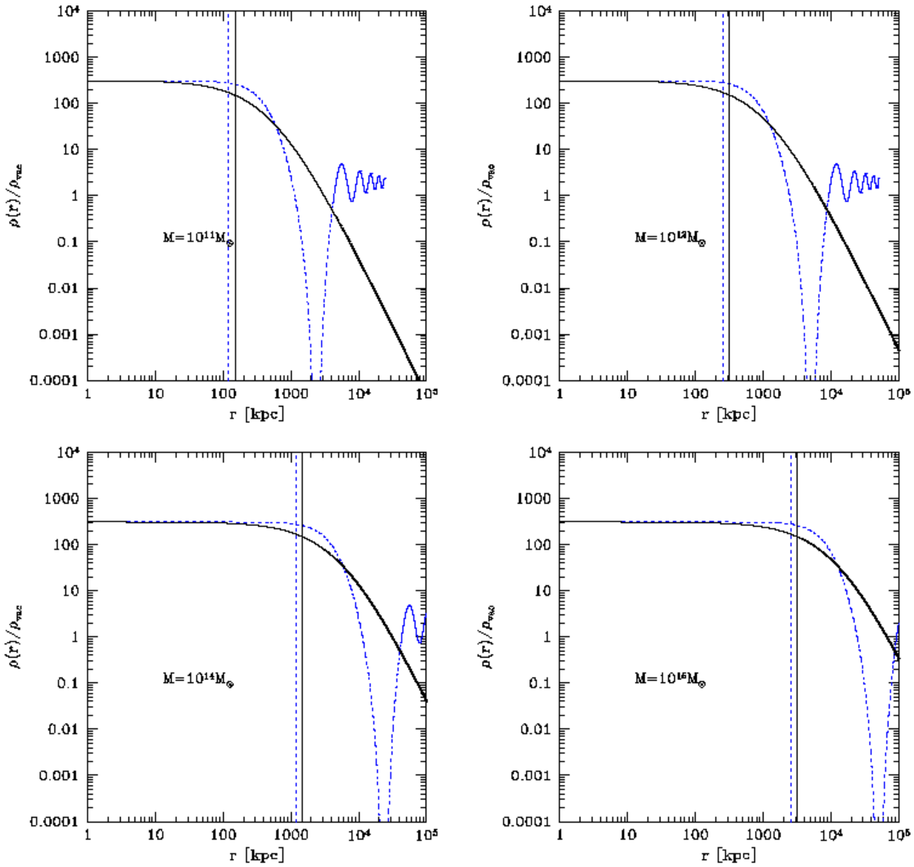

Figure 10. Generalized NFW profile (black solid line) for $m = 0$ compared with the and $n = 3$ ΛLE profile, with its corresponding $\zeta_{\rm crit}$, for different masses.

we find a reasonable agreement between both approaches for the polytropic index $n = 3$ and restricting ourselves to the virial radius. Our model does not have the the undesired features of the cuspy behaviour of the NFW profiles.

The importance of the astrophysical properties and configurations found in this article is that they are specific features to the existence of a dark energy component. Hence, such configurations (e.g, low density configurations) or properties, if ever found in nature would imply a strong evidence for the presence of a dark energy component. Such observations would be a completely independent, and so complementary, of other cosmological probes of dark energy such as Supernova Ia or the CMBR.

ACKNOWLEDGMENTS

We acknowledge Stefanie Phleps for her comments on the manuscript. DFM acknowledge support from the A. Humboldt Foundation.

REFERENCES

Aldrovandi, R., Barbosa, A., L., Crispino, L., C., B. et al., Class. Quant. Grav. **16** 495-506 (1999)

Arieli Y., Rephaeli Y., New Astronomy **8**, 517-528, 2003.

Balaguera-Antolínez, A., Nowakowski, M., Astron. Astrophys **441**, 23 (2005)

Balaguera-Antolínez, A., Nowakowski, M., AIP Conf. Proc. **861**, 1001 (2006), arXive: astro-ph/0603624

Balaguera-Antolínez, A.,Böhmer, C., Nowakowski, M., Int. J. Mod. Phys **D14**, 9, 1507-1526 (2005)

Balaguera-Antolínez, A.,Böhmer, C., Nowakowski, M, Class. Quant. Grav **23**, 485-496 (2006)

Balaguera-Antolínez, A., Mota, D., F., Nowakowski, M., Class. Quant. Grav **23**, 4497-4510 (2006)

Baryshev, Yu., Chernin, A., and Teerikorpi, P., Astron. Astrophys. **378**, 729 (2001)

Binney, J & Tremaine, S., *Galactic Dynamics*, Princeton University Press, 1987

Blake, C., and Glazebrook, K., Astrophys. J. **594**, 665 (2003)

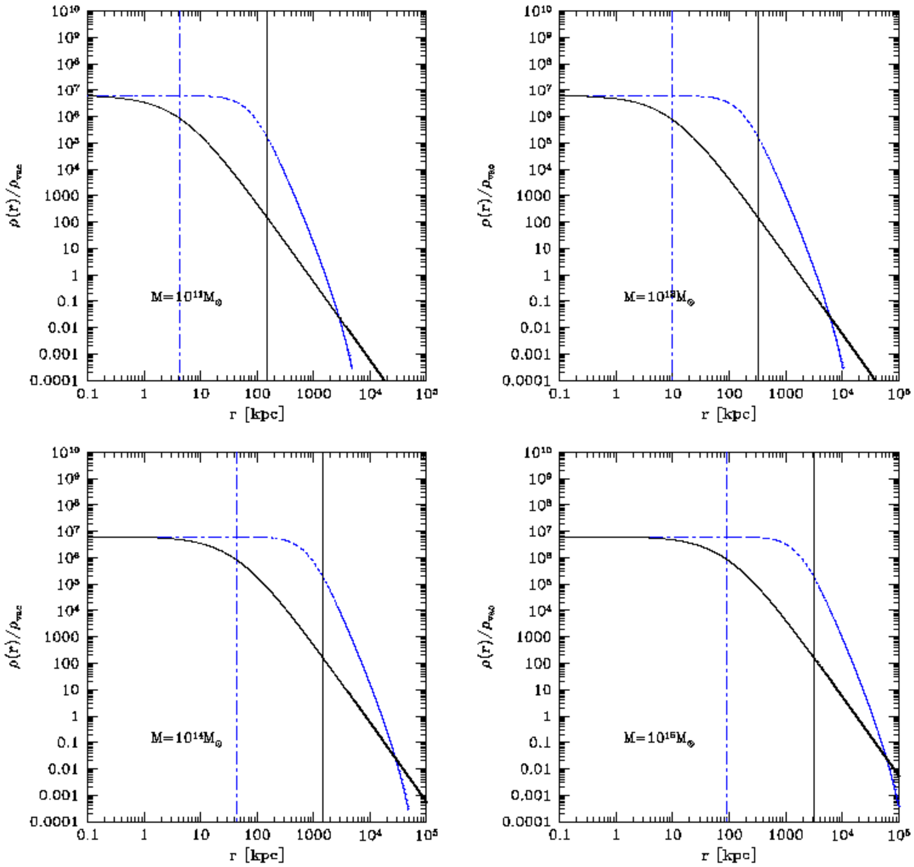

Figure 11. Same as fig 10 for $n = 4.9$

Börner, G., *The Early Universe*, 4th edition, Springer, 2004

Böhmer, C. G., Gen. Rel. Grav. **36**, 1039 (2004)

Böhmer, C. G. & Harko T., Phys. Rev. **D71**, 084026 (2005), arXiv: astro-ph/0509874

Brookfield, A., et al. Phys. Rev. Lett. **96**, 061301 (2006)

Cabral-Roseti, L.G., Matos T., Núẽz D., Sussman R., Zavala J., arXive:astro-ph/0405242.

Caimmi R., arXive:gr-qc/0608030v1

Caldwell, R. R., Phys. Lett. B **545**, 23 (2002)

Cardoso, V. & Gualtieri, L., Class. Quant. Grav. **23**, 7151 (2006)

Chandrasekhar, S. *An Introduction to the Study of Stellar Structure*, Dover Publications, 1967.

Chavanis, P., Astron. Astrophys. **381**, 340 (2002), arXive: astro-ph/0103159

Chen G, and Ratra B, 2004 Astrophys. J. **612**, L1

Chernin, A. D., Nagirner, D. I., Starikova, S. V., Astron. Astrophys. **399**, 19 (2003)

Chernin *et al.*, arXiv:0704.2753 [astro-ph].

Daly, R., A., and Djorgovski, S., G., Astrophys.J. **612**, 652 (2004)

Daly, R., A., and Djorgovski, S., G., Astrophys. J. **597**, 9 (2003)

Debnath U., Nath, S., Chakraborty, S., Mon. Not. Roy. Astron. Soc., **369**, 1961 (2006)

Debatissta, V.P. and Sellwood, J. A., Astropys. J. **493**, L5 (1998)

Dehnen, H. and Rose, B., Astrophys. Space science **207**, 133 (1993)

Diemand J., Kuhlen M., Madau P., submitted to Astron. Astrophys. ArXive: astro-ph/0703337

Dolgov A. D., Hansen S.H., Astropart.Phys. **16**, 339-344 (2002)

Eckehard W., Schunck F., arXiv: gr-qc/9801063

Einstein, A. Straus E. G., Rev. Mod. Phys **17**, 2 and 3, 1945

Gentile G.F., Tononi C., Salucci P., Accepted in Astron. Astrophys , arXive:astro-ph/0701550.

Gibbons, G.W., Patricot C.E., Class.Quant.Grav. **20**, 5223 (2003)

Gonzalez-Casado, G. at al. in Proceedings IAU Colloqium No. **195** (2004)

Gruzinov, A., Astrophys. J, **498**, 458 (1998), arXiv: astro-ph/9705026

Herrera, L., Barreto, W., Gen.Rel.Grav. **36** 127-150 (2004), arXiv:gr-qc/0309052
Henriksen, R. N., Mon.Not.Roy.Astron.Soc. **355**, 1217 (2004)
Hoeft, M¿, Mücket, J. P. and Gottl—"ober, S., Astrophys. J. **602**, 162 (2004)
Hogan, C. J. and Dalcanton, J. J., Phys. Rev. **D62**, 063511 (2000)
Horedt, G. P., Publ. Astron. Soc. Japan, **52**, 217 (2000)
Horellou C, and Berge J., 2005, Mon. Not. Roy. Astron. Soc. **360**, 1393
Iorio, L., Int.J.Mod.Phys. **D15** 473-476 (2006), arXiv:gr-qc/0511137
Jackson J., 1970, Mon. Not. Roy. Astro. Soc. 148, 249
Jetzer P., astro-ph/9609068
Jetzer, P. and Serena, M., Phys. Rev. **D73**, 044015 (2006)
Kaniadakis, C., Lavagno, A., Quarati, P., Phys.Lett. **B369** 308-312 (1996) arXiv: astro-ph/9603109
Kagramanova, V., Kunz, J. and Laemmerzahl, C., Phys. Lett. **B634**, 465 (2006)
Kawano, Y., Oguri, M., Matsubara, T., Ikeuchi, S., Publ.Astron.Soc.Jap. **56** 253-260 (2004)
Kennedy, D., Bludman, S., Astrophys. J. **525** :1024-1031 (1999)
Koivisto T., and Mota D.F., Phys. Rev. D **73** (2006) 083502 [arXiv:astro-ph/0512135].
Koivisto T, & Mota, D., F., Phys. Rev. D **75** (2007a) 023518 [arXiv:hep-th/0609155].
Koivisto T., and Mota D.F., Phys. Lett. B **644** (2007) 104
Koivisto T., and Mota D.F., (2007b) arXiv:0707.0279 [astro-ph].
Lahav O., et al.,Mon.Not.Roy.Astron.Soc **251**, 128-136 (1991)
Lai, C., W,. arXiv: gr-qc/0410040
Lattanzi M., Ruffini R., Vereshchagin G., AIP Conf.Proc. **668** (2003) 263-287
Lombardi, M., Bertin, G., Astron. Astrophys **375**, 1091-1099 (2001), arXiv: astro-ph/0106336
Lynden-Bell D., Wood R., Mon.Not.Roy.Astron.Soc. **138**, 495 (1968)
Maccio A., Mon.Not.Roy.Astron.Soc. **361**, 1250-1256 (2005), arXiv:astro-ph/0402657
Manera, M. and Mota, D. F., Mon.Not.Roy.Astron.Soc. **371** 1373 (2006), arXiv:astro-ph/0504519
Maor I., Lahav O., arXiv:astro-ph/0505308
Matos, T., Nunez, D. and Sussman, R., Gen. Relat. Gravit. **37**, 769 (2005)
Mota, D. F. and van de Bruck, C., Astron. Astrophys. **421**, 71 (2004)
Mota D. F. and Shaw D. J., 2007, Phys. Rev. D 75, 063501;
Mota D. F. and Shaw D. J., 2006, Phys.Rev.Lett.97:151102
McKee, C. F. in ASP Conf. Proc. **243** (2001)
Mukhopadhyay, U., Ray S., arXiv: astro-ph/0510550
Natarajan P., Lynden-Bell D., Mon.Not.Roy.Astron.Soc. **286**, 268-270 (1997)
Navarro, J.S., Frenk, C.S., White, S.D.M., Astrophys. J **462**, 563 (1996)
Noerdlinger P., Petrosian V., Astrophys. J, **168**, 1 (1971)
Nojiri S., Odinstov S. D., Phys.Rev. **D72** (2005) 023003, arXiv: hep-th/0505215
Nowakowski, M., Int. J. Mod. Phys., **D10**, 649 (2001)
Nowakowski, M., Sanabria, J.-C., and Garcia, A., Phys. Rev. **D66**, 023003 (2002)
Nunes, N. J. and Mota, D. F., Mon. Not. Roy. Astron. Soc. 368:2 751 (2006), arXive: astro-ph/0409481
Padmananbhan, T., *Structure Formation in the Universe*, Cambridge University Press, 1993
Penston M.V., Mon.Not.Roy.Astron.Soc. **144**, 425 (1969)
Pinzon, G., A., Calvo-Mozo, B., arXive: astro-ph/0107428
Ren J., Li,& Shen H.,arXive: astro-ph/0604227
Riess, A. G. *et al.* [Supernova Search Team Collaboration], Astrophys. J. **607** 665 (2004)
Rines, K. et al. Astron.J. **124** (2002) 1266, arXive: astro-ph/0206226
Ruffet, M., Rampp, M., Hanka, H.,Th., Astron. Astrophys **321**, 991-1006 (1997)
Ruffini R., Bonazzola S., Phys. Rev **187**, 5 (1969)
Sadeth, S., Rephaeli, Y., New Astron. **9**, 159-171 (2004)
Seo, H., J., and Eisenstein, D., J., Astrophys.J. **598**, 720 (2003)
Sereno M., Mon.Not.Roy.Astron.Soc. **356**, 937-943 (2005)
Shapiro, S. & Teukolsky, S., *Black Holes, White Dwarfs and Neutron Stars*, Wiley-Interscience Publications, 1983
Sommer-Larsen J., Vedel, H., Hellsten U., Astrophys.J. **500** (1998) 610-618
Spergel D., *et al*, astro-ph/0603449
Spruch L., Rev. Mod. Phys, **63**, 1 (1991)
Shaw D. J. and Mota D. F., 2007, to appear in the Astrophys. J. Suppl. arXiv:0708.0868 [astro-ph]
Sussman R. A. and Hernandez X., 2003, Mon.Not.Roy.Astron.Soc. 345 871.
Tegmark M., *et al.* [SDSS Collaboration], Astrophys. J. **606**, 702 (2004)

Umemura, M. and Ikeuchi, S., Astron. Astrophys. **165**, 1 (1986)
Wang P. Astrophys. J. **640**, 18-21 (2006)
Wang, Y., and Mukherjee P., Astrophys. J. **606**, 654 (2004)
Wang, L., and Steinhardt, P. J., Astrophys. J. **508**, 483 (1998)
Weinberg, S., *Gravitation and Cosmology*, Wiley and Sons, 1972
Yabushita S., Mon.Not.Roy.Astron.Soc. **140**, 109 (1968)
Yepes, G. at al. in Proceedings IAU Colloquim **195** (2004)
Zavala, J., Nunez, D., Sussman, R., Cabral-Rosetti, C. G. and Matos, T., J. Cosmol. Astrpart. Phys. **06**, 008 (2006)

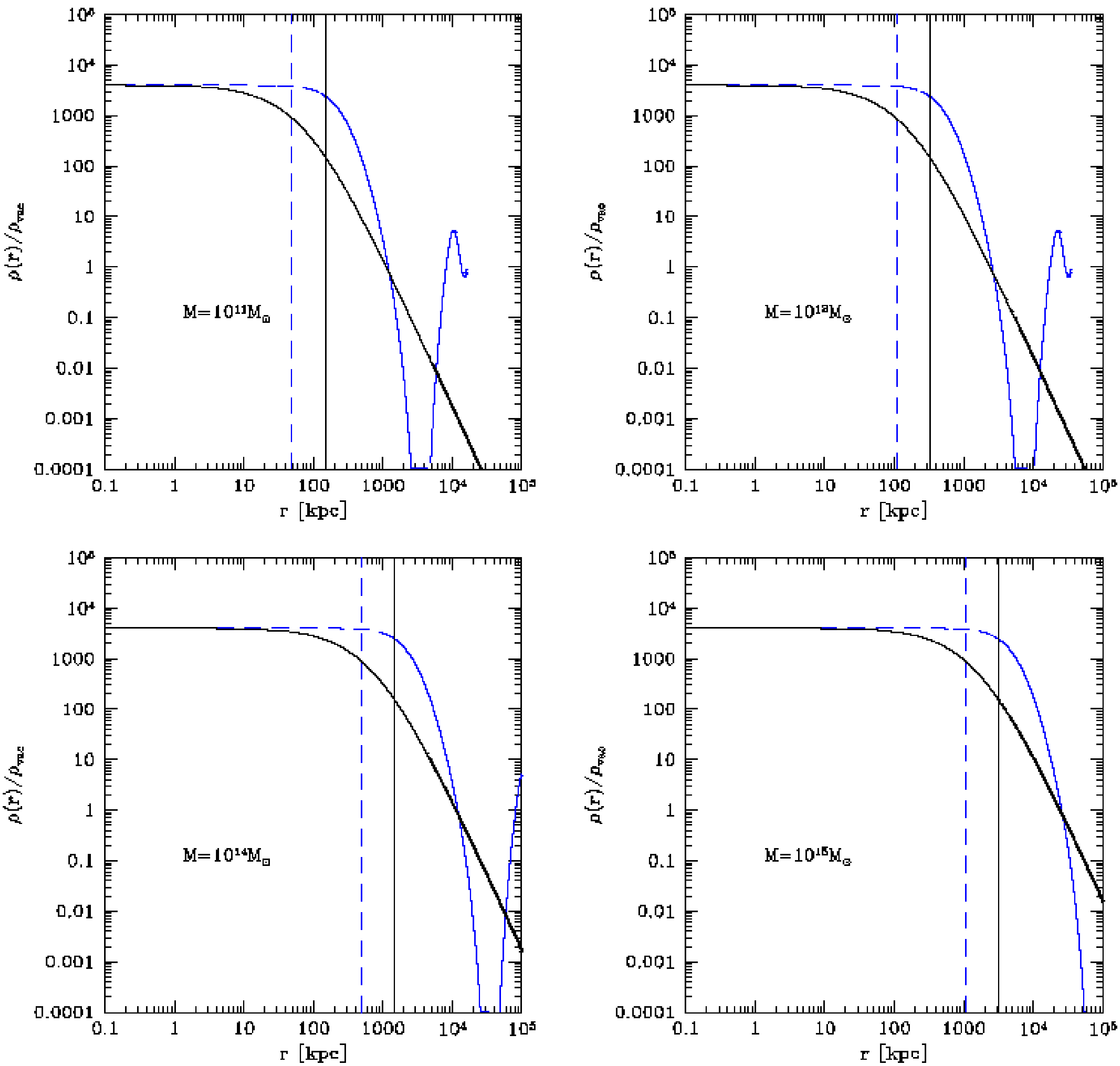

M=10^11 M_⊙
M=10^13 M_⊙
M=10^14 M_⊙
M=10^15 M_⊙
ρ(r)/ρ_vac
r [kpc]

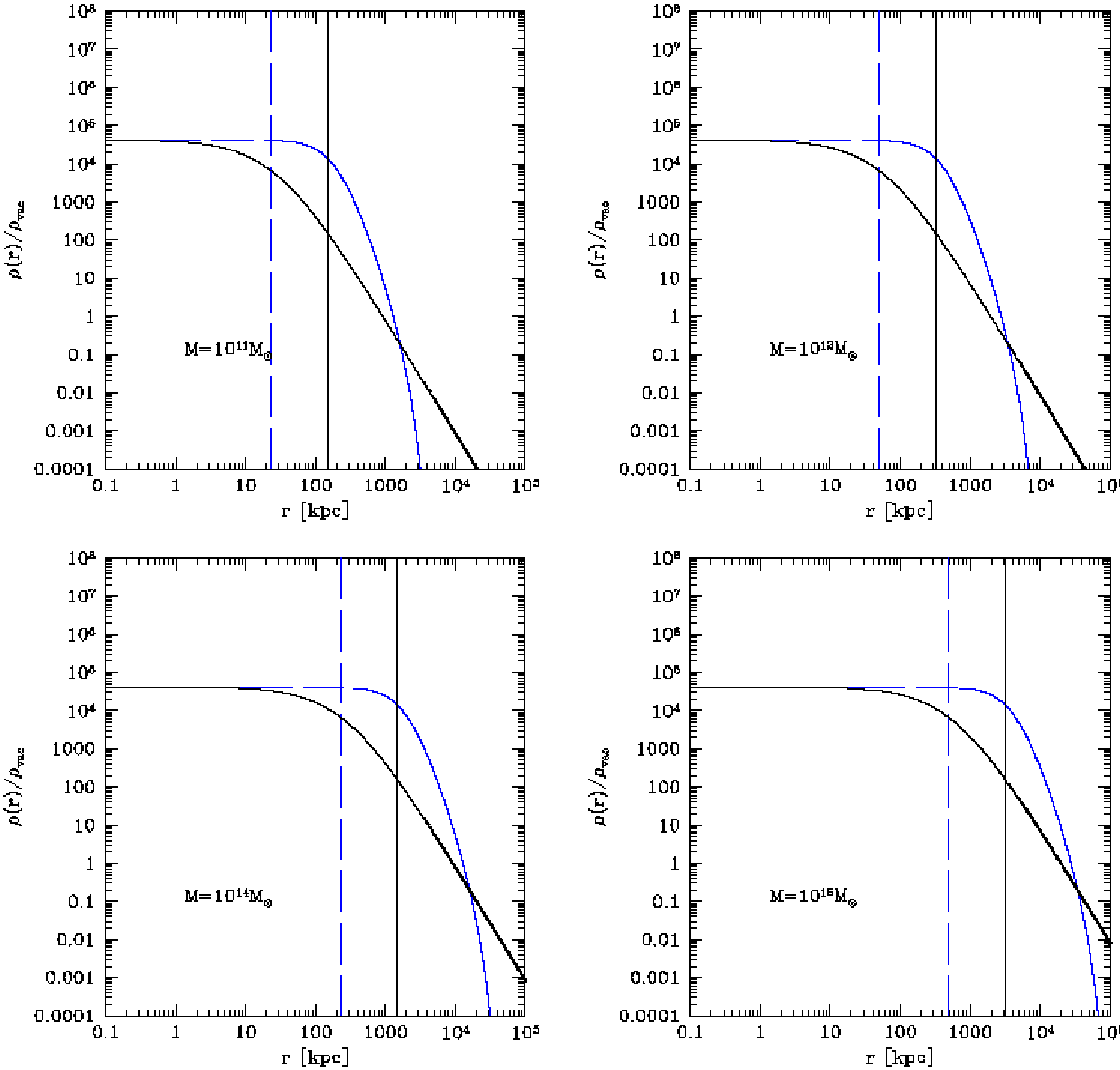

ρ(r)/ρ_vac
r [kpc]
M=10^11 M_⊙
ρ(r)/ρ_vac
r [kpc]
M=10^13 M_⊙
ρ(r)/ρ_vac
r [kpc]
M=10^14 M_⊙
ρ(r)/ρ_vac
r [kpc]
M=10^15 M_⊙